

### ***Remarks***

Reconsideration of this Application is respectfully requested.

Claims 1, 8, and 41 are sought to be amended. Support for the amendments to claims 1 and 41 can be found, *inter alia*, in paragraphs 0003, 0007, and 0099 of the captioned application, and throughout the specification and the claims as originally filed. The amendment to claim 2 was made to improve the syntax of the claim by adding the article "the."

Upon entry of the foregoing amendments, claims 1-41 are pending in the application, with claims 1, 9, 17, 23-25, and 29-41 being the independent claims. In addition, amendments are being made to the specification to reflect the support of government funding and to the title. These changes are believed to introduce no new matter, and their entry is respectfully requested.

Based on the above amendment and the following remarks, Applicants respectfully request that the Examiner reconsider all outstanding objections and rejections and that they be withdrawn.

### ***Restriction/Election***

The Examiner indicated that claims 10-40 were withdrawn from further consideration as being drawn to non-elected inventions. (*See* Paper No. 15, page 2.) The Examiner also recognized that, in Paper No. 9, filed July 8, 2002, Applicants elected Group I (claims 1-16 and 41) without traverse, and that, upon further consideration, the claims of Group I were subject to further restriction in Paper No. 11. *Id.* The Examiner also acknowledged Applicant's traversal of the further restriction and argument that Groups I-IV

should be combined. *Id.* Upon further reconsideration, the Examiner decided to recombine Groups I-IV (claims 1-9 and 41), and examine Groups I-IV together. *Id.*

***Objection to the Title***

The Examiner asserted that the title of the invention is not descriptive. (Paper No. 15, page 2.)

While Applicants believe that the previous title is indicative of the invention to which the claims are directed, solely in an effort to facilitate prosecution of the captioned application, Applicants request that the title be changed to "Methods of Identifying Agents Useful in Treatment of Neurodegenerative Diseases." No new matter is introduced by this change.

Accordingly, the Examiner's objection to the title has been rendered moot, and Applicants respectfully request that the objection to the title be withdrawn.

***Objections to the Claims***

The Examiner objected to claim 8, and suggested that "the syntax of claim 8 can be improved by amending the claim to recite 'is useful in the treatment of.'" (Paper No. 15, page 2.) Applicants have amended claim 8 to recite "is useful in the treatment of."

Claim 41 was objected to "under 37 CFR 1.75(c), as being of improper dependent form for failing to further limit the subject matter of a previous claim." (Paper No. 15, page 2.) Applicants respectfully traverse this objection. Claim 41 is an independent claim. As such, it cannot be of improper dependent form.

The Objections to the claims have been rendered moot or otherwise addressed by the Applicants' amendments and/or remarks, and Applicants respectfully request that the objections to the claims be withdrawn.

***Rejections Under 35 U.S.C. § 112, First Paragraph***

Claims 1-9 and 41 were rejected under 35 U.S.C. § 112, first paragraph because the specification allegedly does not enable one skilled in the art to use the invention commensurate in scope with the claims. (Paper No. 15, page 3.) More specifically, the Examiner asserted that, "while being enabling for a method of identifying compounds which potentiate CCE in cells which comprise various mutants," the specification allegedly "does not reasonably provide enablement for identifying agents useful in the treatment of any and all neurodegenerative diseases." *Id.* Applicants respectfully traverse this rejection.

The specification of the captioned application and the knowledge in the art at the priority date of the captioned application provide sufficient information such that the skilled artisan can practice the full scope of the invention. The specification fully provides how to make and use each aspect of the claimed invention. However, solely in an effort to facilitate prosecution, Applicants have amended independent claims 1 and 41 such that they require identifying an agent capable of treating a neurodegenerative disease associated with amyloid aggregation or neuronal cell death. Although claims 1 (and, therefore, all of its dependent claims) and 41 have been amended as such, Applicants provide the following comments.

The Examiner asserted that:

the breadth of the claims is excessive with regard to intending to treat any and all neurodegenerative diseases with any and all disease-linked mutations. Applicants have only provided

guidance and working examples showing that CCE is clearly altered in specific presenilin mutants.

(Paper No. 15, page 4). The Examiner "concluded that undue experimentation would be required to practice the invention as claimed." *Id.* Applicants respectfully disagree.

According to the Federal Circuit, "[i]t is well settled that patent applicants are not required to disclose every species encompassed by their claims, even in an unpredictable art." *In re Vaeck*, 947 F.2d 488, 496; 20 U.S.P.Q.2d 1438, 1445 (Fed. Cir. 1991) (citing *In re Angstadt*, 537 F.2d 498, 502-03, 190 U.S.P.Q. 214, 218 (CCPA 1976)). Rather, "the disclosure must adequately guide the art worker to determine, without undue experimentation, which species among all those encompassed by the claimed genus possess the disclosed utility." *Id.* "That *some* experimentation may be required is not fatal; the issue is whether the amount of experimentation required is 'undue.'" *Id.* at 495, 20 USPQ2d at 1445 (citing *In re Wands*, 858 F.2d 731, 736-737, 8 USPQ2d (BNA) 1400, 1404 (Fed. Cir. 1988)) (emphasis in original). Factors that may be considered in determining whether experimentation is "undue" were set forth in *Wands*, 858 F.2d at 737, 8 U.S.P.Q.2d at 1404. Among these factors are: the amount of effort involved, the guidance provided by the specification, the presence of working examples, and the level of skill in the art. The test for undue experimentation is not merely quantitative, since a considerable amount of experimentation is permissible, if it is merely routine. *See id.*

Applicants also point out that "[t]he first paragraph of § 112 requires nothing more than objective enablement. How such a teaching is set forth, either by the use of illustrative examples or by broad terminology, is of no importance." *In re Marzocchi*, 439 F.2d 220, 223 (C.C.P.A. 1971).

Claims 1-9 and 41 of the present invention require identifying an agent capable of treating a neurodegenerative disease associated with amyloid aggregation or neuronal cell death.

Applicants have provided working examples demonstrating that the claimed invention is effective. Paragraphs 0077-0080 of the captioned application provide that CCE is reduced in presenilin mutants. Applicants have shown that CCE is dramatically potentiated when the biological activities of mutant presenilins are abolished, and that CCE activity is inversely correlated to presenilin-linked  $\gamma$ -secretase activity (*i.e.*, activity of the enzyme responsible for proteolytic processing of amyloid- $\beta$ -protein precursor (APP), which gives rise to A $\beta$ 42). *See e.g.*, Paragraphs 0011, 0085-0088, and 0092-0093 and Figures 3 and 5, of the Specification.

Applicants have further shown that there is a molecular link between the presenilin FAD-driven changes in the CCE response and alterations in A $\beta$ 42 production. *See* Paragraph 0089 of the specification. Specifically, Applicants have shown that inhibition of the cellular pathways involving CCE specifically increases A $\beta$ 42, which is a molecular phenotype associated with Alzheimer's disease mutant presenilins. *See* Figure 5 and Paragraphs 0090 and 0091 of the captioned application. As provided in Paragraph 0003 of the captioned application, A $\beta$ 42 is a protein species that aggregates and is deposited in senile plaques. Thus, Applicants have shown that mutant presenilins mediate downregulation of CCE, and that decreased CCE results in increased production of the protein which aggregates and forms senile plaques in Alzheimer's disease. They have also shown that abolishing the biological activities of mutant presenilins results in an increase of CCE.

Alzheimer's disease-associated mutations give rise to an increased production of the amyloid  $\beta$  peptide (A $\beta$ 42) in Alzheimer's disease patients, and A $\beta$ 42 aggregates in senile

plaques. *See* Paragraph 0003 of the Specification. It has been confirmed since the present invention that neurodegenerative diseases associated with protein aggregation could have overlapping pathologies, and that a treatment effective for one could be effective for others. *See, e.g.,* Masliah *et al.*, *Proc. Nat. Acad. Sci.* 98: 12245, 12250 (2001) ("the pathogenic interactions between A $\beta$  and hSYN [associated with Parkinson's disease] demonstrated here suggest that drugs aimed at blocking the accumulation of A $\beta$  and hSYN might benefit a broader spectrum of neurodegenerative disorders than previously anticipated.") (attached hereto as Exhibit A); Temussi *et al.*, *EMBO J.* 22: 355, 356 (2003) ("The two disease families [Alzheimer's and poly-Q diseases, which include Huntington's], could therefore share a common mechanism of pathogenesis, in which the aggregates affect the cellular functions, and eventually cause neuronal cell death.") (attached hereto as Exhibit B); Murphy, R.M., *Ann. Rev. Biomed. Eng.* 4: 155 (2002) ("The structural similarities between protein aggregates of dissimilar origin suggest that therapeutic strategies successful against one disease may have broad utility in others.") (attached hereto as Exhibit C). These documents are cited not to enable the claims, but to provide confirmatory evidence that the captioned application provides enablement of the full scope of the invention. Thus, it is clear that the claimed method can be used to identify agents capable of treating a neurodegenerative disease associated with amyloid aggregation or neuronal cell death.

The Examiner further asserted that "Applicants have not demonstrated how these agents would be used to treat Alzheimer's disease or any other neurodegenerative disease, nor would it be predictable to the artisan how to do so." (Paper No. 15, page 4). Applicants respectfully disagree. The specification as originally filed describes in detail how the identified agents would be used to treat neurodegenerative diseases. *See* Paragraphs 0048-

0072 of the Specification. Any variation from this description would require only routine experimentation. The Examiner is also reminded that the claims are directed to a method for *identifying* an agent capable of treating a neurodegenerative disease associated with amyloid aggregation or neuronal cell death, not a method for treating a neurodegenerative disease.

The Examiner's grounds of rejection of claims 1-9 and 41 under 35 U.S.C. § 112, first paragraph have been addressed by Applicants' amendments and/or remarks. Accordingly, the Examiner is respectfully requested to reconsider and withdraw this rejection.

***Rejections Under 35 U.S.C. § 112, Second Paragraph***

Claims 1-9 and 41 were rejected under 35 U.S.C. § 112, second paragraph, as allegedly being indefinite. (Paper No. 15, page 4). More particularly, the Examiner indicated that it is not understood "how identifying an agent which potentiates CCE can be guaranteed to be an agent which is useful in treating any, if not all, neurodegenerative diseases." *Id.* The Examiner indicated that "[this rejection can be overcome by amending the preamble to recite that the agent is potentially useful in the treatment of a neurodegenerative disease." *Id.* Applicants believe that the claim as originally filed, when read in light of the specification, would reasonably apprise one skilled in the art of the metes and bound of the claimed invention; nevertheless, solely in an effort to facilitate prosecution, Applicants have amended the claim to recite "an agent capable of treating" to make explicit that which was implicit. Accordingly, the Examiner's grounds of rejection of claims 1-9 and 41 under 35 U.S.C. § 112, second paragraph, have been rendered moot. Applicants therefore respectfully request the Examiner to reconsider and withdraw this rejection.

***Rejections Under 35 U.S.C. § 102***

Claims 1, 9, and 41 were rejected under 35 U.S.C. §§ 102 (a) and 102 (e) as allegedly being anticipated by Birnbaumer *et al.*, U.S. Patent No. 5,932,741. (*See* Paper No. 15, pages 5 and 6, respectively.) Applicants respectfully traverse this rejection.

Amended claims 1 and 41 recite ". . . identifying an agent capable of treating a neurodegenerative disease associated with amyloid aggregation or neuronal cell death."

The Examiner asserts that "Birnbaumer *et al.* teach a method of identifying compounds which may be useful in controlling CCE in mammalian cells," and that "Birnbaumer *et al.* also teach cells which overexpress TRP." (Paper No. 15, page 5.) The Examiner specifically points out that "[t]he reference does not teach that CCE is linked to degenerative diseases," but cites *Ex parte Novitski*, 26 USPQ2d 1389, 1391 (1993), for the proposition that "the assay (i.e. method steps) would be identical regardless of what the intention of the assay was for." (Paper No. 15, page 5).

While the Examiner characterizes U.S. Patent No. 5,932,741 as teaching "a method of identifying compounds which may be useful in controlling CCE in mammalian cells," and "cells which overexpress TRP," the Examiner specifically states that what U.S. Patent No. 5,932,741 "does *not* teach is that CCE is linked to degenerative diseases." (Paper No. 15, page 5) (emphasis added). Thus, more specifically, the cited document does not teach identifying an agent capable of treating a neurodegenerative disease associated with amyloid aggregation or neuronal cell death as required by claims 1 and 41. Claim 9 depends from claim 1, and therefore "shall be construed to include all the limitations of the claim incorporated by reference." 37 C.F.R. § 1.75 (c).



As a further indication that U.S. Patent No. 5,932,741 does not teach that CCE is linked to neurodegenerative diseases, col. 15, lines 30-44 of that document lists conditions for which controlling calcium ion levels would be useful. There are no neurodegenerative diseases listed among these conditions. Therefore, U.S. Patent No. 5,932,741 does not describe each and every limitation of Applicants' claimed invention such that the subject matter would be recognized by one skilled in the art.

The Examiner also rejected claims 1, 9, and 41 under 35 U.S.C. § 102 (b) as allegedly being anticipated by Birnbaumer *et al.*, *Proc. Natl. Acad. Sci.* 93: 15195-15202 (1996). (Paper No. 15, page 6.) Applicants respectfully traverse this rejection.

According to the Examiner, Birnbaumer *et al.* "teach assays which increase CCE (i.e. CCE was measured)," "a method of identifying compounds which affect CCE," "cells which overexpress TRP," and "the activation of CCE by the agent, IP3." (Paper No. 15, page 6.) However, as the Examiner again explicitly states, "[t]he reference does **not** teach that CCE is linked to neurodegenerative diseases." *Id.* (emphasis added). In fact, neurodegenerative diseases are not even mentioned. As set forth above, claims 1, 9, and 41 require identifying an agent capable of treating a neurodegenerative disease associated with amyloid aggregation or neuronal cell death. Because Birnbaumer *et al.* do not describe identifying an agent capable of treating a neurodegenerative disease associated with amyloid aggregation or neuronal cell death, the document does not describe each and every limitation of Applicants' claimed invention. Therefore, Birnbaumer *et al.* does not anticipate the claimed invention. Accordingly, the rejection is overcome, and Applicants respectfully request that the Examiner reconsider and withdraw the rejection.

The Examiner also rejected claim 1 under 35 U.S.C. § 102 (b) as allegedly being anticipated by Buxbaum *et al.*, U.S. Patent No. 5,538,983, and as allegedly being anticipated by Berridge, *Biochem. J.* 312: 1-11 (1996). (Paper No. 15, pages 5-6.) Applicants respectfully traverse these rejections.

As set forth *supra*, for U.S. Patent No. 5,932,741 and Birnbaumer *et al.*, *Proc. Natl. Acad. Sci.* 93: 15195-15202 (1996), in order for either U.S. Patent No. 5,538,983 or Berridge to anticipate the claimed invention, each document would have to describe each and every limitation of the claimed invention. As with the previously discussed documents, the Examiner explicitly stated that they do not teach that CCE is linked to neurodegenerative diseases. Thus, the cited documents do not teach identifying an agent capable of treating a neurodegenerative disease associated with amyloid aggregation or neuronal cell death as required in claim 1. Because neither U.S. Patent No. 5,538,983 nor Berridge describe identifying an agent capable of treating a neurodegenerative disease associated with amyloid aggregation or neuronal cell death, these documents do not describe each and every limitation of Applicants' claimed invention. Accordingly, Applicants respectfully request the Examiner to reconsider and withdraw the rejection.

### ***Rejections Under 35 U.S.C. § 103***

Claims 1-4, 7-9, and 41 were rejected under 35 U.S.C. § 103 (a) as allegedly being unpatentable over Kim *et al.* ("The N141I Presenilin 2 Familial Alzheimer Mutation is Associated with Abated Proteasomal Degradation and Reduced Capacitative Calcium Entry," published in the *Soc. Neurosci. 29<sup>th</sup> Annual Meeting 25*: Abstract 1568:629.6, Society for Neuroscience (October 1999), "the Kim *et al.* abstract"), in view of Birnbaumer *et al.* (*Proc.*

*Nat'l. Acad. Sci.* 93: 15195-15202, "Birnbaumer *et al.* PNAS"). (Paper No. 15, page 7.) Claims 1 and 5 were rejected under 35 U.S.C. § 103 (a) as allegedly being unpatentable over the Kim *et al.* abstract in view of Birnbaumer *et al.* PNAS and further in view of Gibson *et al.*, *Neurobiol. of Aging* 18: 573-580 (1997). (Paper No. 15, page 8.) Claims 1 and 6 were rejected under 35 U.S.C. § 103 (a) as allegedly being unpatentable over the Kim *et al.* abstract in view of Birnbaumer *et al.* PNAS and further in view of Masliah *et al.*, *Prog. Neurobiol.* 50: 493-503 (1996). (Paper No. 15, pages 8-9.) Applicants respectfully traverse these rejections.

The Kim *et al.* abstract was published in October of 1999, less than one year before the Applicants' priority date of March 22, 2000. (*See* page 1 of Specification as originally filed.) As such, the determination of whether or not the Kim *et al.* abstract is considered prior art would be made under 35 U.S.C. § 102 (a). *See* M.P.E.P. § 2141.01, (8<sup>th</sup> ed., Rev.1, Feb. 2003) ("Subject matter that is prior art under 35 U.S.C. 102 can be used to support a rejection under section 103.") (citing *Ex parte Andresen*, 212 USPQ 100, 102 (Bd. Pat. App. & Inter. 1981)). A rejection under 35 U.S.C. § 102 (a) can be overcome by showing that a document's disclosure was derived from applicants' own work. M.P.E.P. § 2132.01, (8<sup>th</sup> ed., Rev. 1, Feb. 2003) ("The rejection can also be overcome by submission of a specific declaration by the applicant establishing that the article is describing applicant's own work.") (quoting *In re Katz*, 687 F.2d 450, 215 USPQ 14 (CCPA 1982)).

Submitted herewith is a Declaration under 37 C.F.R. § 1.132, by Dr. Tae-Wan Kim, Dr. Rudolph E. Tanzi, and Andrew S. Yoo, stating that the Kim *et al.* abstract was co-authored by all of, and none other than, the inventors named in the captioned application, and that the abstract is a description of their own work. Therefore, the Kim *et al.* abstract cannot

be used as 35 U.S.C. § 102 (a) art for the rejection under 35 U.S.C. § 103 (a). The other cited documents, Birnbaumer *et al.*, PNAS, Gibson *et al.*, and Berridge, do not, themselves, support the rejections under 35 U.S.C. § 103 (a). Accordingly, Applicants respectfully request that the Examiner reconsider and withdraw these rejections.

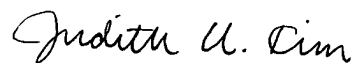
### ***Conclusion***

All of the stated grounds of objection and rejection have been properly traversed, accommodated, or rendered moot. Applicants therefore respectfully request that the Examiner reconsider all presently outstanding objections and rejections and that they be withdrawn. Applicants believe that a full and complete reply has been made to the outstanding Office Action and, as such, the present application is in condition for allowance. If the Examiner believes, for any reason, that personal communication will expedite prosecution of this application, the Examiner is invited to telephone the undersigned at the number provided.

Prompt and favorable consideration of this Amendment and Reply is respectfully requested.

Respectfully submitted,

STERNE, KESSLER, GOLDSTEIN & FOX P.L.L.C.



Judith U. Kim  
Attorney for Applicants  
Registration No. 40,679

Date: October 14, 2003  
1100 New York Avenue, N.W.  
Washington, D.C. 20005-3934  
(202) 371-2600

::ODMA\MHODMA\SKGF\_DC1;186214;2

# $\beta$ -Amyloid peptides enhance $\alpha$ -synuclein accumulation and neuronal deficits in a transgenic mouse model linking Alzheimer's disease and Parkinson's disease

Eliezer Masliah<sup>\*,†</sup>, Edward Rockenstein<sup>\*</sup>, Isaac Veinbergs<sup>†</sup>, Yutaka Sagara<sup>\*</sup>, Margaret Mallory<sup>\*</sup>, Makoto Hashimoto<sup>\*</sup>, and Lennart Mucke<sup>§</sup>

Departments of <sup>\*</sup>Neurosciences and <sup>†</sup>Pathology, University of California at San Diego, La Jolla, CA 92093; and <sup>§</sup>Gladstone Institute of Neurological Disease and Department of Neurology, University of California, San Francisco, CA 94141

Communicated by Robert W. Mahley, The J. David Gladstone Institutes, San Francisco, CA, August 6, 2001 (received for review May 8, 2001)

Alzheimer's disease and Parkinson's disease are associated with the cerebral accumulation of  $\beta$ -amyloid and  $\alpha$ -synuclein, respectively. Some patients have clinical and pathological features of both diseases, raising the possibility of overlapping pathogenetic pathways. We generated transgenic (tg) mice with neuronal expression of human  $\beta$ -amyloid peptides,  $\alpha$ -synuclein, or both. The functional and morphological alterations in doubly tg mice resembled the Lewy-body variant of Alzheimer's disease. These mice had severe deficits in learning and memory, developed motor deficits before  $\alpha$ -synuclein singly tg mice, and showed prominent age-dependent degeneration of cholinergic neurons and presynaptic terminals. They also had more  $\alpha$ -synuclein-immunoreactive neuronal inclusions than  $\alpha$ -synuclein singly tg mice. Ultrastructurally, some of these inclusions were fibrillar in doubly tg mice, whereas all inclusions were amorphous in  $\alpha$ -synuclein singly tg mice.  $\beta$ -Amyloid peptides promoted aggregation of  $\alpha$ -synuclein in a cell-free system and intraneuronal accumulation of  $\alpha$ -synuclein in cell culture.  $\beta$ -Amyloid peptides may contribute to the development of Lewy-body diseases by promoting the aggregation of  $\alpha$ -synuclein and exacerbating  $\alpha$ -synuclein-dependent neuronal pathologies. Therefore, treatments that block the production or accumulation of  $\beta$ -amyloid peptides could benefit a broader spectrum of disorders than previously anticipated.

**A**ging is a major risk factor for neurodegenerative disorders, such as Alzheimer's disease (AD) and Parkinson's disease (PD), and the number of people with these conditions is increasing rapidly. In the United States alone, an estimated 4 million people have AD and at least one million have PD. Within the next 40–50 years, these numbers are projected to increase to over 8 million for AD and to 4 million for PD. Each neurodegenerative disease appears to have a predilection for specific brain regions and cell populations. However, human cases with clinical and neuropathological features of both AD and PD (1–3) raise the possibility that these diseases involve overlapping pathways.

Many AD patients develop signs of PD and some PD patients become demented (3). Both diseases are associated with degeneration of neurons and interneuronal synaptic connections, depletion of specific neurotransmitters, and abnormal accumulation of misfolded proteins, whose precursors participate in normal central nervous system functions (4–11). The  $\beta$ -amyloid protein precursor (APP) and  $\alpha$ -synuclein (SYN) are expressed abundantly in synapses, are well conserved across species, and have been implicated in neural plasticity, learning, and memory (6, 7, 12). Mutations in human APP (hAPP) that increase production of hAPP-derived  $\beta$ -amyloid peptides (A $\beta$ ) cause autosomal dominant forms of familial AD (FAD) (11), and expression of FAD-mutant hAPPs in neurons of transgenic (tg) mice results in the age-dependent development of AD-like

central nervous system alterations (13–17). Mutations in human SYN (hSYN) that enhance hSYN aggregation have been identified in autosomal dominant forms of PD (18, 19). Although most patients with AD and PD have no mutations in hAPP or hSYN, even the most frequent “sporadic” forms of these diseases are associated with an abnormal accumulation of A $\beta$  (10, 11) and hSYN (20–22), respectively. A $\beta$  accumulates in extracellular amyloid plaques and probably also inside neurons, and hSYN accumulates in intraneuronal inclusions called Lewy bodies transgenic mice expressing wild-type hSYN in neurons develop neuronal accumulations of hSYN, loss of dopaminergic terminals in the basal ganglia, and motor impairments (23), all of which are hallmarks of PD. Neuronal expression of hSYN in fruit flies resulted in similar alterations (24). That neuronal accumulation of hSYN is associated with similar morphological and functional alterations in species as diverse as flies, mice, and humans is provocative and suggests that it may contribute to the development of PD and other Lewy-body diseases.

We hypothesized that hSYN and A $\beta$  have distinct, as well as convergent, pathogenic effects on the integrity and function of the brain. hSYN might affect motor function more than cognitive function, whereas the opposite might be true for A $\beta$ . In addition, hSYN and A $\beta$  could interact more directly by engaging synergistic neurodegenerative pathways. To test these hypotheses, we generated tg mice that express hSYN either alone or in combination with hAPP/A $\beta$ .

## Methods

**Generation and Behavioral Testing of Tg Mice.** Heterozygous hSYN mice from line D (23) were crossed with heterozygous hAPP mice from line J9 (17). The offspring were genotyped (17, 23) and analyzed at 4–22 months of age. Before behavioral experiments, mice were singly housed to reduce effects of social stress. Mice had free access to food and water. Experiments were carried out during the light cycle. Locomotor activity was analyzed as described (23). Spatial learning and memory were assessed in a water maze test. A pool (diameter, 180 cm) was filled with opaque water (24°C), and mice were first trained to locate a visible platform (days 1–6) and then a submerged hidden platform (days 7–12) in three daily trials 2–3 min apart. Mice that failed to find the hidden platform within 90 s were put on it for 30 s. The same platform location was used for all sessions and all

Abbreviations: AD, Alzheimer's disease; PD, Parkinson's disease; APP,  $\beta$ -amyloid protein precursor; SYN,  $\alpha$ -synuclein; hAPP, human APP; A $\beta$ ,  $\beta$ -amyloid peptides; FAD, familial AD; hSYN, human SYN; ChAT, choline acetyltransferase; SIPT, synaptophysin-immunoreactive presynaptic terminals of defined signal intensity; tg, transgenic.

<sup>†</sup>To whom reprint requests should be addressed. E-mail: emasliah@ucsd.edu.

The publication costs of this article were defrayed in part by page charge payment. This article must therefore be hereby marked “advertisement” in accordance with 18 U.S.C. §1734 solely to indicate this fact.

mice. The starting point at which each mouse was placed into the water was changed randomly between two alternative entry points located at a similar distance from the platform. Time to reach the platform (latency), path length, and swim speed were recorded with a Noldus Instruments EthoVision video tracking system (San Diego Instruments, San Diego) set to analyze two samples per second. On day 13, the platform was removed for a 30-s probe trial, during which we recorded the percent time the mouse spent in the quadrant of the pool that previously contained the platform (target quadrant) and in each of the nontarget quadrants. To control for differences in motivation or fatigue, the probe trial was followed by a trial with a visible platform. There were no significant differences in average swim speeds or path lengths between the different groups of mice during the latter trial (data not shown).

**Quantitation of Transgene Products.** hSYN and hAPP mRNA and protein levels were determined by RNase protection assay and Western blot analysis as described (23, 25), except the actin riboprobe was complementary to nucleotides 490–565 of mouse  $\beta$ -actin cDNA (GenBank accession no. X03672), and an actin antibody (MAB1501, Chemicon) was used to confirm equal loading of protein in the Western blot analysis.

For the determination of A $\beta$  levels by ELISA, samples of mouse cortex were homogenized in ice-cold PBS containing 5 M guanidine-HCl and 1 $\times$  protease inhibitor mixture (pH 8.0) (Calbiochem). Homogenates were mixed for 3–4 h at room temperature and centrifuged at 16,000  $\times$  g for 20 min at 4°C. The supernatant was diluted 10-fold in Dulbecco's PBS (pH 7.4) containing 5% BSA and 0.03% Tween 20. A $\beta$ 1–40 and A $\beta$ 1–42 levels in the diluted brain homogenates were quantitated with a sandwich ELISA (BioSource International, Camarillo, CA) according to the manufacturer's instructions.

**Neuronal Cell Culture.** Cells of the immortalized hypothalamic neuronal cell line GT1–7 (a gift from P. Mellon, University of California at San Diego) express neuronal markers, form synapses, produce neurotransmitters (26) and, on transfection with SYN, show mitochondrial alterations, inclusion body formation, evidence of oxidative stress, and synaptic dysfunction (27). Cells were stably transfected with SYN cDNA or control plasmid as described (27), plated in 24-well plates coated with poly-L-lysine ( $5 \times 10^4$ /0.5 ml of DMEM with 10% serum and without G418), and treated with synthetic peptides from Sigma as outlined in Fig. 6. For quantitation of SYN-immunoreactive inclusions, coverslips were immunostained (27) and analyzed by light microscopy and computer-aided image analysis with a Quantimet 570C (Leica, Deerfield, IL). For each condition, five coverslips and an average of 20 cells per coverslip were analyzed. Results were expressed as percentage of cells with SYN-immunoreactive inclusions.

**Neuropathological Analysis.** Mice were euthanized by transcardial saline perfusion under anesthesia with chloral hydrate. Brains were removed and divided sagittally. The right hemisphere was snap-frozen and stored at –70°C for RNA or protein analysis. The left hemisphere was drop-fixed in phosphate-buffered 4% paraformaldehyde at 4°C for 48 h and serially sectioned sagittally at 40  $\mu$ m with a Vibratome 2000 (Leica).

Immunohistochemical analysis was performed on free-floating Vibratome sections (17, 23) with anti-hSYN (72–10, 1:200) (23), anti-hAPP (clone 8E5, 1:1000, Elan Pharmaceuticals, San Francisco) (13), anti-A $\beta$  (3D6, 1:600, Elan Pharmaceuticals) (28), anti-choline acetyltransferase (ChAT; AB143, 1:1000, Chemicon), and anti-synaptophysin (SY38, 1:10, Chemicon). The specificity of immunostaining results was confirmed by incubating sections or cells overnight with preimmune serum or without primary antibody. For double-labeling, sections were

incubated overnight at 4°C with anti-hSYN (1:1000), followed by detection with the Tyramide Signal Amplification-Direct (Red) system (1:100, NEN Life Sciences). Sections were then incubated overnight with anti-A $\beta$  (1:100), followed by incubation with FITC-conjugated avidin (1:75, Vector Laboratories).

The density of ChAT-positive neurons and of neurons with hSYN-immunoreactive inclusions was determined morphometrically. Two immunoperoxidase-stained sections were analyzed per mouse and antigen, and four light microscopic images (0.1 mm<sup>2</sup> each) were acquired per section. The threshold was set to detect only positively stained cells, and objects were counted automatically with the Quantimet 570C. The results from eight images per mouse were averaged and expressed as numbers per mm<sup>2</sup>. The area occupied by 3D6-immunoreactive A $\beta$  deposits was quantitated as described (17). Three immunolabeled sections were analyzed per mouse, and the average of the individual measurements was used to calculate group means.

Confocal microscopy was carried out as described (23) with a Zeiss 63 $\times$  (numerical aperture 1.4) objective on an Axiovert 35 microscope (Zeiss) mounted on a MRC1024 laser scanning confocal microscope (Bio-Rad). The average percent area occupied by synaptophysin-immunoreactive presynaptic terminals of defined signal intensity (SIPT) was determined as described (17). Three sections were analyzed per mouse and four confocal images (7, 282  $\mu$ m<sup>2</sup> each) of the neocortex and of the caudate/putamen per section.

Some Vibratome sections were postfixed with 2% glutaraldehyde/0.1% osmium tetroxide in 0.1 M sodium cacodylate buffer, embedded in epoxy, and analyzed with a Zeiss EM10 electron microscope as described (23). For immunogold cytochemistry (14), Vibratome sections were fixed in 0.25% glutaraldehyde and 3% paraformaldehyde in 0.1 M cacodylate buffer (pH 7.4). From each mouse, the temporal cortex was dissected and placed in gelatin capsules containing a polymerized layer of LR white (medium grade, Ted Pella, Redding, CA). Blocks were sectioned with an Ultracut E, and thin sections (60–90 Å) were placed on nickel grids coated with 0.5% Parlodion film. Grids were incubated with anti-A $\beta$  (3D6) or anti-hSYN (72–10) followed by rabbit anti-mouse-gold or goat anti-rabbit-gold (5 nm, Zymed), respectively. Immunogold-labeled grids were examined with a Zeiss EM10 electron microscope. In control experiments, grids were incubated with gold-labeled secondary antibodies in the absence of primary antibody.

**Statistics.** Mice, sections, and samples were analyzed in a blind-coded fashion. Statistical analyses were performed with STATVIEW 5.0 (SAS Institute, Cary, NC). Null hypotheses were rejected at the 0.05 level.

## Results and Discussion

**Coexpression of hSYN and hAPP in Vivo.** Heterozygous tg hSYN mice and hAPP mice (Fig. 1*a* and *b*) with high levels of neuronal hSYN (line D) (23) or A $\beta$  (line J9) (17) production, respectively, were crossed to obtain four groups of littermates: hSYN mice ( $n = 26$ ), hAPP mice ( $n = 32$ ), hSYN/hAPP mice ( $n = 21$ ), and non-tg controls ( $n = 31$ ). Levels of transgene-derived mRNAs in the brain were similar in singly and doubly tg mice (Fig. 1*c*), indicating that coexpression of hSYN and hAPP did not alter transgene expression. At the protein level, expression of hSYN did not affect hAPP expression in doubly tg mice (Fig. 1*d*). Cerebral hSYN levels tended to be higher in hSYN/hAPP mice than in hSYN mice (Fig. 1*d*). In addition, the levels of apparent hSYN oligomers and larger hSYN aggregates were higher in hSYN/hAPP mice than in hSYN mice (Fig. 1*d* and data not shown).

**Neurological Deficits in hSYN/hAPP Mice.** Motor deficits were assessed with the rotarod test as described (23). At 6 months of age,

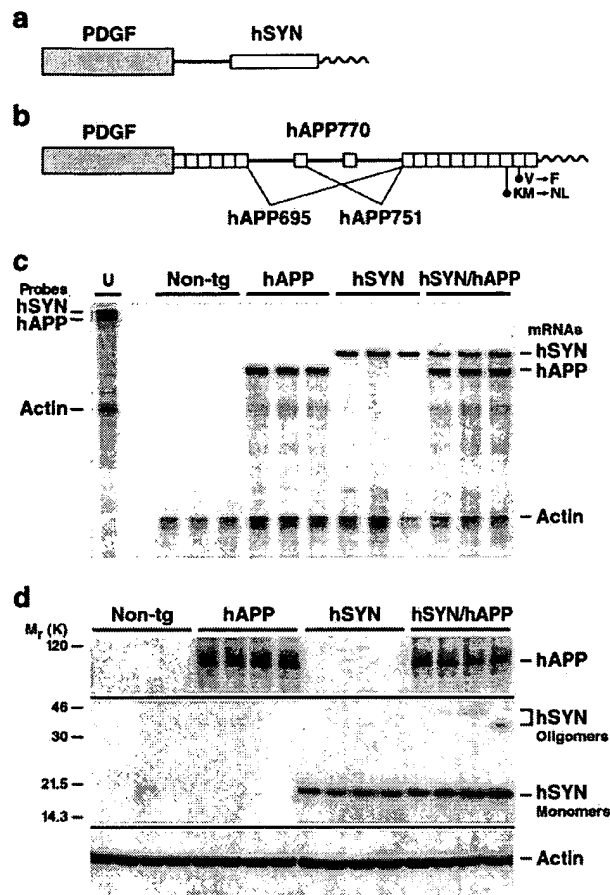


**Fig. 1.** Expression of hSYN and hAPP in brains of tg mice. (a and b) Neuronal expression of a hSYN cDNA (a) and an alternatively spliced hAPP minigene (b) was directed by the human platelet-derived growth factor  $\beta$ -chain promoter as described (17, 23, 25). Elements are not drawn to scale. hSYN/hAPP doubly tg mice were obtained from crosses between previously established lines: hSYN line D (23) and hAPP line J9 (17, 50). Line J9 carries familial Alzheimer's disease (FAD)-linked mutations (670/671<sub>KM</sub>→NL and 717<sub>V</sub>→F, hAPP770 numbering) that increase the production of A $\beta$ 1–40 and A $\beta$ 1–42. (c) Cerebral levels of transgene-derived mRNAs. Total RNA was extracted from hemibrains of 4-month-old mice and analyzed by RNase protection assay. The leftmost lane shows signals of undigested radiolabeled riboprobes (U). The lanes to the right contained the same riboprobes plus brain RNA (10  $\mu$ g per lane) from different mice, digested with RNases. Protected mRNA segments are identified on the right. Signals were quantitated by phosphorimager analysis: singly and doubly tg mice ( $n = 3$  per genotype) did not differ significantly in hSYN/actin ( $0.77 \pm 0.11$  vs.  $0.82 \pm 0.25$ ) or hAPP/actin ( $1.60 \pm 0.27$  vs.  $1.33 \pm 0.21$ ) ratios (mean  $\pm$  SD). (d) Cerebral levels of hAPP, hSYN, and mouse actin. Frontal cortex homogenates of 4-month-old mice ( $n = 4$  per genotype) were separated into cytosolic (for hSYN) and particulate (for hAPP) fractions (12  $\mu$ g per lane), resolved by SDS/10% PAGE, and subjected to Western blot analysis as described (23). hSYN was detected with 72–10 (1:1000) and hAPP with 8E5 (1:2500). Blots were cropped as indicated by horizontal lines. Anti-actin (MAB1501, 1:500) labeling of stripped hSYN (not shown) and hAPP (bottom) blots confirmed equal loading of lanes. Longer exposures of the full-length hSYN blot revealed apparent hSYN oligomers, as well as higher molecular weight hSYN aggregates, in hSYN/hAPP mice and, at much lower levels, also in hSYN singly tg mice (data not shown).

hSYN/hAPP mice already showed significant deficits relative to non-tg controls ( $P < 0.03$  by repeated measures ANOVA), whereas hSYN mice did not (Fig. 2a). At 12 months of age, both hSYN/hAPP and hSYN mice showed deficits in this test com-

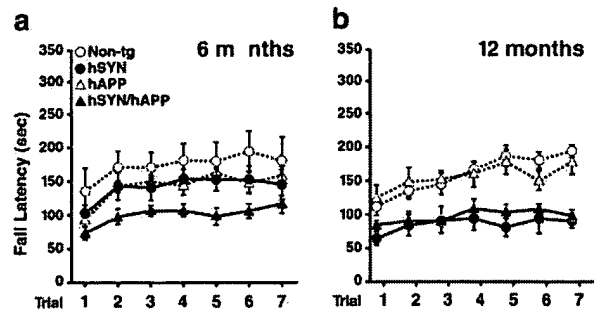


**Fig. 2.** hAPP/A $\beta$  accelerates hSYN-dependent motor deficits. Male mice, 6 (a) or 12 (b) months of age ( $n = 6$ –8 per age and genotype), were assessed in the rotarod test as described (23). After an initial adaptation period, fall latencies were recorded in seven consecutive trials (10-min intertrial intervals). Compared with age-matched non-tg controls, only hSYN/hAPP mice were significantly impaired at 6 months whereas both hSYN and hSYN/hAPP mice were impaired at 12 months.

pared with non-tg controls ( $P < 0.001$  by repeated-measures ANOVA) (Fig. 2b). hAPP mice had no significant motor deficits at either age. The severity of motor deficits was similar in 6-month-old hSYN/hAPP and 12-month-old hSYN and hSYN/hAPP mice, suggesting that hAPP/A $\beta$  accelerates the development of hSYN-dependent motor deficits.

To determine the effects of hSYN and hAPP/A $\beta$  on spatial learning and memory, we assessed the mice in a water maze test (Fig. 3). All groups of mice were able to locate a visible platform equally well (Fig. 3a), indicating that the motor deficits of hSYN/hAPP do not preclude normal performance in this test. In the hidden platform sessions, mice must use their memory of visual cues outside of the maze to find the submerged platform. In these sessions, hSYN/hAPP mice showed the most significant learning deficits, whereas hSYN mice and non-tg controls performed normally (Fig. 3a). The probe trial, during which the platform is removed, provides a putative measure of spatial memory retention. In this trial, hSYN/hAPP mice and hAPP

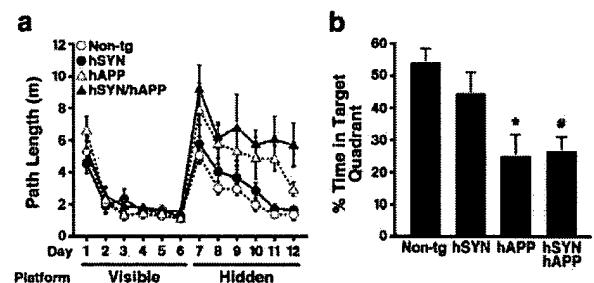


**Fig. 3.** hSYN/hAPP mice have severe learning deficits in the water maze test. (a) Six-month-old male mice ( $n = 6$  per genotype) were first trained for 6 days to find a visible platform. All groups of mice acquired this task equally well, demonstrating that the motor deficits observed at this age in hSYN/hAPP mice (Fig. 2) did not interfere with their performance in the water maze test. On day 7 of training, the platform was hidden under the opaque water to test the ability of the mice to use visual cues outside of the maze to locate the hidden platform. Non-tg and hSYN mice learned to locate the hidden platform, whereas hAPP mice were impaired ( $P = 0.023$  vs. non-tg by repeated-measures ANOVA). hSYN/hAPP mice had even more significant difficulties learning this task ( $P = 0.0094$  vs. non-tg by repeated-measures ANOVA). (b) After removal of the platform for a probe trial on day 13, hAPP and hSYN/hAPP mice spent less time searching in the target quadrant than non-tg controls, consistent with impaired retention of spatial memory. \*,  $P < 0.05$  vs. non-tg mice (Tukey–Kramer test). #,  $P < 0.05$  vs. non-tg mice (Student Newman–Keuls test).

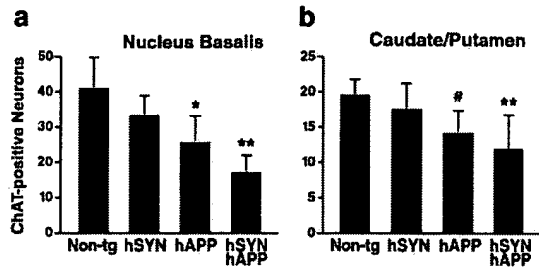


**Fig. 4.** Loss of cholinergic neurons in hAPP and hSYN/hAPP mice. Brain sections ( $n = 2$  per mouse) of 20- to 22-month-old mice ( $n = 3-7$  per genotype) were labeled with an antibody to ChAT, and the nucleus basalis (a) and caudate/putamen (b) were analyzed by light microscopy and morphometry. For each mouse, eight images were analyzed, and the results were used to calculate the average number of immunostained cells per mm<sup>2</sup> (mean  $\pm$  SD). \*,  $P < 0.05$ ; \*\*,  $P < 0.01$  vs. non-tg controls (Tukey–Kramer test); #,  $P < 0.05$  vs. non-tg controls (Student Newman–Keuls test).

mice showed significantly less preference for the target quadrant than non-tg controls, suggesting impaired memory retention; hSYN mice were not impaired (Fig. 3b).

These results indicate that the motor deficits of hSYN/hAPP mice are caused primarily by hSYN, whereas their deficits in spatial learning and memory are caused primarily by hAPP/A $\beta$ . Similar effects of hSYN and hAPP/A $\beta$  may contribute to Lewy-body diseases, which also combine motor and cognitive deficits.

**Age-Dependent Neurodegeneration.** Degeneration of cholinergic neurons in the nucleus basalis of Meynert results in acquisition deficits in the water maze task in rodents (29). It is also a potentially important determinant of cognitive decline in AD and Lewy-body diseases (30, 31). ChAT mediates the synthesis of acetylcholine and serves as a marker of cholinergic neurons. We determined the density of ChAT-immunoreactive neurons in the nucleus basalis of our tg models ( $n = 13-17$  mice/genotype, age range: 4–22 months). Simple regression analysis revealed a significant correlation between aging and loss of ChAT-positive neurons in hSYN mice ( $r = 0.6$ ,  $P < 0.03$ ), hAPP mice ( $r = 0.66$ ,  $P < 0.01$ ), and hSYN/hAPP mice ( $r = 0.86$ ,  $P < 0.0001$ ), but not in non-tg controls ( $r = 0.22$ ,  $P > 0.4$ ). The greatest loss was observed in aged hSYN/hAPP mice (Fig. 4a), which had fewer ChAT-positive neurons than aged hAPP mice ( $P < 0.03$  by unpaired Student's  $t$  test). These results are consistent with the observation that cholinergic deficits are more severe in human patients with the Lewy-body variant of AD than in patients with pure AD (30). hSYN/hAPP mice and hAPP mice also had a significant loss of cholinergic neurons in the caudate/putamen (Fig. 4b), consistent with the decreased ChAT activity in the caudate of AD patients with or without Lewy bodies (30).

People with AD or the Lewy-body variant of AD typically also develop a significant loss of synapses in the neocortex, which is reflected in decreased synaptophysin immunoreactivity (31–33). We measured SIPT in the neocortex of 4- to 20-month-old mice ( $n = 15-19$  per genotype). There was a significant negative correlation between aging and neocortical SIPT levels in hAPP mice ( $r = 0.744$ ,  $P = 0.0006$ ) and hSYN/hAPP mice ( $r = 0.524$ ,  $P = 0.021$ ), but not in hSYN mice ( $r = 0.479$ ,  $P = 0.071$ ) or non-tg controls ( $r = 0.151$ ,  $P = 0.564$ ). At 20 months of age, SIPT levels in the neocortex (percent area occupied, mean  $\pm$  SD,  $n = 3-4$  mice/genotype) were highest in non-tg controls ( $25.6 \pm 0.9$ ) and lowest in hSYN/hAPP mice ( $18.3 \pm 4.8$ ,  $P < 0.05$  by Tukey–Kramer test), with values for hAPP mice ( $20.9 \pm 1.7$ ) and hSYN mice ( $23.0 \pm 0.9$ ) in between. In contrast, SIPT levels in the caudate/putamen at 20 months were normal in non-tg mice ( $27.1 \pm 1.5$ ) and hAPP mice ( $25.1 \pm 3.6$ ), but decreased in hSYN

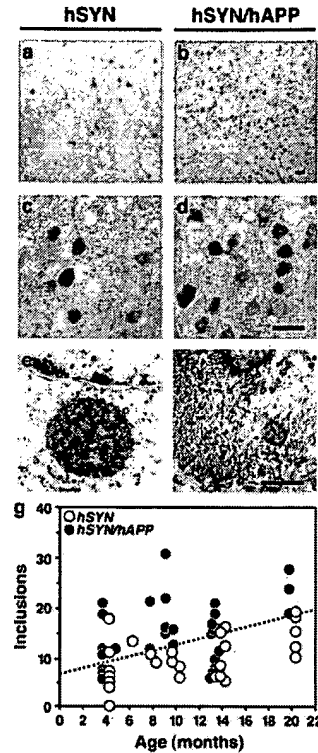


**Fig. 5.** Increased number and fibrillar characteristics of neuronal inclusions in hSYN/hAPP mice. (a–d) Brain sections were labeled with an antibody against hSYN (72–10) and analyzed by light microscopy. hSYN/hAPP mice (b and d) had more hSYN-immunoreactive neuronal inclusions in the temporal cortex (depicted here) and in the cingulate cortex (not shown) than hSYN mice (a and c). Images are from 12-month-old mice. (Scale bars, 20  $\mu$ m.) (e and f) Sections of temporal cortex from 12-month-old hSYN (e) or hSYN/hAPP (f) mice were analyzed by transmission electron microscopy. Images depict intraneuronal inclusions. (Scale bar, 1  $\mu$ m.) (g) hSYN-immunoreactive neuronal inclusions increased with age in both hSYN ( $r = 0.51$ ,  $P = 0.006$ ) and hSYN/hAPP ( $r = 0.39$ ,  $P = 0.027$ ) mice. Each dot represents measurements obtained in the temporal cortex of a different mouse expressed as average number of hSYN-immunoreactive inclusions per mm<sup>2</sup>.

mice ( $21.0 \pm 0.9$ ) and hSYN/hAPP mice ( $20.1 \pm 1.7$ ) ( $P < 0.05$  vs. non-tg controls by Tukey–Kramer test).

Thus, the age-dependent loss of cholinergic neurons in hSYN/hAPP mice depends primarily on hAPP/A $\beta$ , with hSYN having some additive effects in the nucleus basalis. The age-dependent loss of SIPT in the neocortex of these mice is also due primarily to hAPP/A $\beta$  with minor contributions from hSYN. Loss of SIPT in the basal ganglia is due almost entirely to hSYN.

**A $\beta$  Promotes Accumulation of hSYN.** Accumulation of hSYN within neurons is a hallmark of Lewy-body diseases, including the Lewy-body variant of AD. An age-dependent accumulation of hSYN occurs in neurons of hSYN singly tg mice (23). Between 4 and 20 months of age, the number of neuronal inclusions in the neocortex was on average 1.6-fold higher in hSYN/hAPP mice than in age-matched hSYN mice ( $15.3 \pm 1.1$  vs.  $9.5 \pm 0.9$  per mm<sup>2</sup>,  $n = 28-32$  mice per genotype, mean  $\pm$  SEM,  $P = 0.0002$  by unpaired two-tailed Student's  $t$  test). This is illustrated for 12-month-old mice in Fig. 5a–d. The number of inclusions increased with age in both hSYN and hSYN/hAPP mice (Fig. 5g). These results indicate that hAPP/A $\beta$  enhances the accumulation of hSYN in neurons.

By ultrastructural analysis, all intraneuronal inclusions in



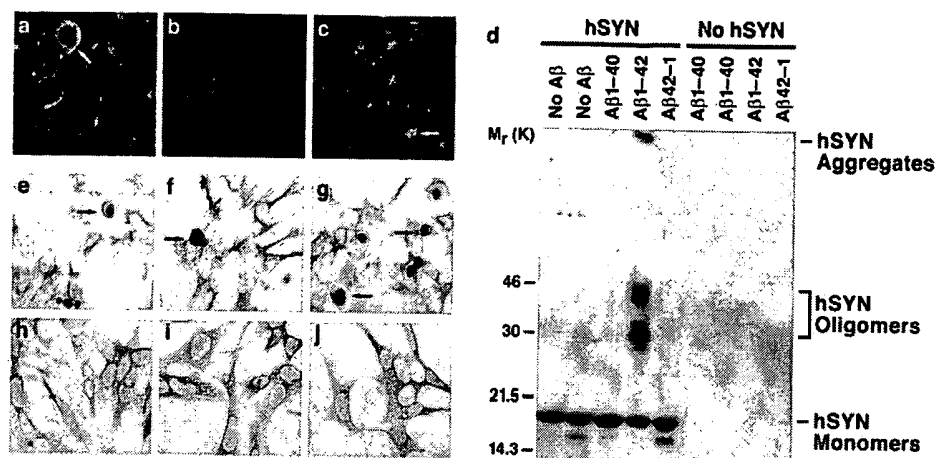


**Fig. 6.** Role of hAPP/A $\beta$  in the accumulation of hSYN *in vivo* and *in vitro*. (a–c) Sections of temporal cortex from 12-month-old hSYN/hAPP (a and c) or hAPP (b) mice were double-labeled with antibodies against hSYN (red) and hAPP (green) (a and b) or against hSYN (red) and A $\beta$  (green) (c) and analyzed by confocal microscopy. Note the colabeling for hAPP and hSYN (yellow) of the neuron (arrow) containing a dense hSYN accumulation (a) and the close association of A $\beta$  deposits (green granules) with intracellular hSYN accumulations (red) (c). All images were obtained at a magnification of  $\times 930$ . The image in c was magnified electronically to better visualize A $\beta$ -immunoreactive granules. (d) Recombinant hSYN (10  $\mu$ M final concentration) was or was not mixed with freshly solubilized synthetic A $\beta$ 1–40, A $\beta$ 1–42, or control peptide of reverse sequence (A $\beta$ 42–1) (each at a final concentration of 10  $\mu$ M) in 20  $\mu$ l of 100 mM Tris-HCl buffer (pH 7.5). All samples were incubated at 37°C for 24 h and then subjected to SDS/15% PAGE. After blotting of samples onto nitrocellulose membrane, the membrane was blocked with Tris-buffered saline (TBS; 20 mM Tris-HCl, pH 7.5/150 mM NaCl) containing 3% BSA, followed by incubation with anti-hSYN (1:1000) in TBS containing 1% BSA. The membrane was then incubated with  $^{125}$ I-labeled protein A (ICN), followed by autoradiography. (e–j) Neuronal GT1–7 cells stably transfected with SYN cDNA (e–g) or control plasmid (h–j) as described (27), were left untreated (e and h) or exposed for 48 h to A $\beta$ 1–40 (f and i), A $\beta$ 1–42 (g and j), or A $\beta$ 42–1 (not shown) at 2  $\mu$ M final concentration, followed by immunoperoxidase staining with anti-SYN (27).

hSYN mice were amorphous and electrodense (Fig. 5e, and ref. 23), whereas  $\approx 15\%$  of the intraneuronal inclusions in hSYN/hAPP were fibrillar (Fig. 5f), increasing their resemblance to Lewy bodies in the human condition (34, 35). Filamentous inclusions in the neuronal cytoplasm were labeled when brain sections of hSYN/hAPP mice were analyzed by immunogold electron microscopy with anti-hSYN or anti-A $\beta$  (data not shown). These results suggest that A $\beta$  may promote the *in vivo* fibrillization of hSYN by direct interaction. Further supporting this possibility, A $\beta$ -immunoreactive granular deposits were detected by confocal microscopy in hSYN-positive intraneuronal inclusions in hSYN/hAPP mice (Fig. 6c).

To further evaluate whether the alterations observed in hSYN/hAPP mice could indeed result from direct interactions between A $\beta$  and hSYN, we extended our *in vivo* analysis to two *in vitro* models. In a cell-free system, A $\beta$ 1–42 strongly promoted the formation of presumed hSYN oligomers and high molecular weight hSYN polymers (Fig. 6d), consistent with previous observations (36). This effect was observed with both aged (putatively aggregated) and freshly solubilized A $\beta$ 1–42. However, because A $\beta$ 1–42 aggregates rapidly in aqueous solutions, we cannot be certain that the effect was independent of the aggregation state of A $\beta$ 1–42. Interestingly, the less fibrillogenic A $\beta$ 1–40 did not affect hSYN aggregation *in vitro* (Fig. 6d).

A $\beta$ 1–42 and A $\beta$ 1–40 also had different effects on the intracellular accumulation of SYN in neuronal cell cultures when added to the culture medium (Fig. 6e–j). The percentage of cells with SYN-immunoreactive inclusions was higher in cultures treated with A $\beta$ 1–42 ( $55.4 \pm 10.3$ ) than in untreated cultures ( $21.4 \pm 6.4$ ) or cultures treated with A $\beta$ 1–40 ( $19.9 \pm 4.8$ ) or A $\beta$ 42–1 ( $19.4 \pm 5.2$ ) (mean  $\pm$  SD,  $P < 0.05$  by Tukey–Kramer test).

Overproduction of A $\beta$ 1–42 within the endoplasmic reticulum and intermediate compartment (10) may interfere with the processing of SYN, enhancing its accumulation. However, our cell culture data demonstrate that extracellular exposure to A $\beta$ 1–42 is sufficient to induce the intracellular accumulation of

SYN, whereas exposure to A $\beta$ 1–40 is not. Interestingly, cellular uptake of extracellular A $\beta$ 1–42, but not A $\beta$ 1–40, disrupted the integrity of lysosomal membranes (37, 38). Moreover, the association of soluble SYN with planar lipid bilayers results in extensive bilayer disruption (39). The combined action of A $\beta$ 1–42 and SYN could cause endosomal–lysosomal membranes to leak, allowing for direct interactions between A $\beta$ 1–42 and SYN in the cytosol. As demonstrated by our *in vitro* findings, such an interaction could promote the intracellular accumulation of SYN. This effect of A $\beta$ 1–42 on SYN might be mediated by direct fibrillogenic interactions between these molecules (40) or by free radicals. A $\beta$  may exert oxidative stress (41), and growing evidence suggests that oxidative crosslinking of SYN contributes to Lewy-body formation (9, 42). These possibilities are not mutually exclusive and deserve to be tested further in future studies.

In contrast to the prominent effects of A $\beta$  on SYN accumulation, hSYN expression did not significantly alter the extracellular deposition of A $\beta$  into plaques or the development of plaque-associated neuritic dystrophy in 8-, 12-, or 20-month-old hSYN/hAPP mice compared with age-matched hAPP mice ( $n = 3$ –4 mice per genotype and age). Twelve-month-old hAPP mice and hSYN/hAPP mice had similar cerebral levels of A $\beta$ 1–40 ( $4.3 \pm 0.88$  vs  $4.6 \pm 0.6$ ) and A $\beta$ 1–42 ( $248 \pm 48$  vs  $275 \pm 41$ ) as determined by ELISA ( $\mu$ g/g of hemibrain, mean  $\pm$  SD,  $n = 4$ –11 mice per genotype).

## Conclusions

hSYN/hAPP mice have cognitive and motor alterations, loss of cholinergic neurons and SIPT, extensive amyloid plaques, and hSYN-immunoreactive intraneuronal fibrillar inclusions. All of these features are also found in the Lewy-body variant of AD (2, 30, 43, 44). Interestingly,  $\approx 25\%$  of patients with AD develop frank parkinsonism (3), and hSYN-immunoreactive Lewy-body-like inclusions develop in most cases of sporadic AD and FAD, as well as in Down's syndrome, which is associated with early onset AD (45, 46). Moreover, Lewy bodies contain hAPP

(47–49). Our study demonstrates that hSYN and hAPP/A $\beta$  have distinct, as well as convergent, pathogenic effects on the integrity and function of the brain. Although hSYN did not affect the A $\beta$ -dependent development of neuritic plaques or the overall A $\beta$  content in the brain, it worsened hAPP/A $\beta$ -dependent cognitive deficits and neurodegeneration in specific brain regions. These findings indicate that hSYN may enhance the plaque-independent neurotoxicity of A $\beta$  (17, 50, 51). They help explain the clinical observation that the Lewy-body variant of AD causes a more rapid cognitive decline than pure AD (30).

Overexpression of hAPP/A $\beta$ , in turn, promoted the intra-neuronal accumulation of hSYN and accelerated the development of motor deficits in tg mice. Although we cannot be certain whether these effects were mediated by A $\beta$  or another hAPP product, our *in vitro* studies strongly suggest that A $\beta$ 1–42 is the predominant culprit. It remains to be determined whether the neuronal deficits in these models and the corresponding human diseases are dependent on fibrillar or prefibrillar forms of A $\beta$  and hSYN (17, 50–52). In either case, the pathogenic interac-

tions between A $\beta$  and hSYN demonstrated here suggest that drugs aimed at blocking the accumulation of A $\beta$  or hSYN might benefit a broader spectrum of neurodegenerative disorders than previously anticipated.

**Note Added in Proof.** Since the acceptance of our paper, two reports have appeared demonstrating that A $\beta$ 1–42 promotes the aggregation of tau into neurofibrillary tangles (53, 54). These results are consistent with the effects of A $\beta$ 1–42 on  $\alpha$ -synuclein aggregation we identified in the current study. Taken together, these findings suggest that A $\beta$ 1–42 might contribute to diverse conformational diseases.

We thank Pamela Mellon for the GT1–7 cell line, Peter Seubert and Dora Games for antibodies against APP and A $\beta$ , Steve Finkbeiner and Fen-Biao Gao for helpful comments on the manuscript, John Carroll for preparation of graphics, Stephen Ordway and Gary Howard for editorial assistance, and Denise McPherson for administrative assistance. This work was supported by National Institutes of Health Grants AG11385, AG5131, AG10869, and AG18440, and Zenith Award from the Alzheimer's Association (to L.M.).

- Ditter, S. M. & Mirra, S. S. (1987) *Neurology* 37, 754–760.
- Hansen, L., Salmon, D., Galasko, D., Masliah, E., Katzman, R., DeTeresa, R., Thal, L., Pay, M. M., Hofstetter, R. & Klauber, M. (1990) *Neurology* 40, 1–8.
- Galasko, D., Hansen, L. A., Katzman, R., Wiederholt, W., Masliah, E., Terry, R., Hill, L. R., Lessin, P. & Thal, L. J. (1994) *Arch. Neurol.* 51, 888–895.
- Terry, R. D., Katzman, R., Bick, K. L. & Sisodia, S. S. (1999) *Alzheimer Disease* (Lippincott, Philadelphia).
- Lang, A. E. & Lozano, A. M. (1998) *N. Engl. J. Med.* 339, 1044–1143.
- Seabrook, G. R., Smith, D. W., Bowery, B. J., Easter, A., Reynolds, T., Fitzjohn, S. M., Morton, R. A., Zheng, H., Dawson, G. R., Sirinathsinghji, D. J. S., et al. (1999) *Neuropharmacology* 38, 349–359.
- Clayton, D. F. & George, J. M. (1998) *Trends Neurosci.* 21, 249–254.
- Goedert, M., Spillantini, M. G. & Davies, S. W. (1998) *Curr. Opin. Neurobiol.* 8, 619–632.
- Giasson, B. I., Duda, J. E., Murray, I. V. J., Chen, Q. P., Souza, J. M., Hurtig, H. I., Ischiropoulos, H., Trojanowski, J. Q. & Lee, V. M. Y. (2000) *Science* 290, 985–989.
- Wilson, C. A., Doms, R. W. & Lee, V. M.-Y. (1999) *J. Neuropathol. Exp. Neurol.* 58, 787–794.
- Selkoe, D. J. (2001) *Physiol. Rev.* 81, 741–766.
- Huber, G., Bailly, Y., Martin, J. R., Mariani, J. & Brugg, B. (1997) *Neuroscience* 80, 131–320.
- Games, D., Adams, D., Alessandrini, R., Barbour, R., Berthelette, P., Blackwell, C., Carr, T., Clemens, J., Donaldson, T., Gillespie, F., et al. (1995) *Nature (London)* 373, 523–527.
- Masliah, E., Sisk, A., Mallory, M., Mucke, L., Schenk, D. & Games, D. (1996) *J. Neurosci.* 16, 5795–5811.
- Price, D. L. & Sisodia, S. S. (1998) *Annu. Rev. Neurosci.* 21, 479–505.
- Dodart, J. C., Meziane, H., Mathis, C., Bales, K. R., Paul, S. M. & Ungerer, A. (1999) *Behav. Neurosci.* 113, 982–990.
- Mucke, L., Masliah, E., Yu, G.-Q., Mallory, M., Rockenstein, E. M., Tatsuno, G., Hu, K., Kholodenko, D., Johnson-Wood, K. & McConlogue, L. (2000) *J. Neurosci.* 20, 4050–4058.
- Polymeropoulos, M. H., Lavedan, C., Leroy, E., Ide, S. E., Dehejia, A., Dutra, A., Pike, B., Root, H., Rubenstein, J., Boyer, R., et al. (1997) *Science* 276, 2045–2047.
- Krüger, R., Kuhn, W., Müller, T., Woitalla, D., Graeber, M., Kösel, S., Przuntek, H., Epplen, J. T., Schöls, L. & Riess, O. (1998) *Nat. Genet.* 18, 106–108.
- Spillantini, M. G., Schmidt, M. L., Lee, V. M.-Y., Trojanowski, J. Q., Jakes, R. & Goedert, M. (1997) *Nature (London)* 388, 839–840.
- Wakabayashi, K., Matsumoto, K., Takayama, K., Yoshimoto, M. & Takahashi, H. (1997) *Neurosci. Lett.* 239, 45–48.
- Takeda, A., Mallory, M., Sundsmo, M., Honer, W., Hansen, L. & Masliah, E. (1998) *Am. J. Pathol.* 152, 367–372.
- Masliah, E., Rockenstein, E., Veinbergs, I., Mallory, M., Hashimoto, M., Takeda, A., Sagara, Y., Sisk, A. & Mucke, L. (2000) *Science* 287, 1265–1269.
- Feany, M. B. & Bender, W. W. (2000) *Nature (London)* 404, 394–398.
- Rockenstein, E. M., McConlogue, L., Tan, H., Gordon, M., Power, M., Masliah, E. & Mucke, L. (1995) *J. Biol. Chem.* 270, 28257–28267.
- Mellon, P. L., Windle, J. J., Goldsmith, P. C., Padula, C. A., Roberts, J. L. & Weiner, R. I. (1990) *Neuron* 5, 1–10.
- Hsu, L. J., Sagara, Y., Arroyo, A., Rockenstein, E., Sisk, A., Mallory, M., Wong, J., Takenouchi, T., Hashimoto, M. & Masliah, E. (2000) *Am. J. Pathol.* 157, 401–410.
- Johnson-Wood, K., Lee, M., Motter, R., Hu, K., Gordon, G., Barbour, R., Khan, K., Gordon, M., Tan, H., Games, D., et al. (1997) *Proc. Natl. Acad. Sci. USA* 94, 1550–1555.
- Mandel, R. J., Gage, F. H. & Thal, L. J. (1989) *Exp. Neurol.* 104, 208–217.
- Langlais, P. J., Thal, L., Hansen, L., Galasko, D., Alford, M. & Masliah, E. (1993) *Neurology* 43, 1927–1934.
- Samuel, W., Alford, M., Hofstetter, C. R. & Hansen, L. (1997) *J. Neuropathol. Exp. Neurol.* 56, 499–508.
- Terry, R. D., Masliah, E., Salmon, D. P., Butters, N., DeTeresa, R., Hill, R., Hansen, L. A. & Katzman, R. (1991) *Ann. Neurol.* 30, 572–580.
- Brown, D. F., Risser, R. C., Bigio, E. H., Tripp, P., Stiegler, A., Welch, E., Eagan, K. P., Hladik, C. L. & White, C. L. I. (1998) *J. Neuropathol. Exp. Neurol.* 57, 955–960.
- Kuzuhara, S., Mori, H., Izumiyama, N., Yoshimura, M. & Ihara, Y. (1988) *Acta Neuropathol.* 75, 345–353.
- Serpell, L. C., Berriman, J., Jakes, R., Goedert, M. & Crowther, R. A. (2000) *Proc. Natl. Acad. Sci. USA* 97, 4897–4902.
- Paik, S. R., Lee, J.-H., Kim, D.-H., Chang, C.-S. & Kim, Y.-S. (1998) *FEBS Lett.* 421, 73–76.
- Yang, A. J., Chandswangbhuvana, D., Margol, L. & Glabe, C. G. (1998) *J. Neurosci. Res.* 52, 691–698.
- Yang, A. J., Chandswangbhuvana, D., Shu, T., Henschen, A. & Glabe, C. G. (1999) *J. Biol. Chem.* 274, 20650–20656.
- Jo, E. J., McLaurin, J., Yip, C. M., St. George-Hyslop, P. & Fraser, P. E. (2000) *J. Biol. Chem.* 275, 34328–34334.
- El-Agnaf, O. M. A. & Irvine, G. B. (2000) *J. Struct. Biol.* 130, 300–309.
- Varadarajan, S., Yatin, S., Aksenova, M. & Butterfield, D. A. (2000) *J. Struct. Biol.* 130, 184–208.
- Hashimoto, M., Hsu, L. J., Xia, Y., Takeda, A., Sisk, A., Sundsmo, M. & Masliah, E. (1999) *NeuroReport* 10, 717–721.
- McKeith, I. G., Galasko, D., Kosaka, K., Perry, E. K., Dickson, D. W., Hansen, L. A., Salmon, D. P., Lowe, J., Mirra, S. S., Byrne, E. J., et al. (1996) *Neurology* 47, 1113–1124.
- Bancher, C., Braak, H., Fischer, P. & Jellinger, K. A. (1993) *Neurosci. Lett.* 162, 179–182.
- Lippa, C. F., Schmidt, M. L., Lee, V. M. Y. & Trojanowski, J. Q. (1999) *Ann. Neurol.* 45, 353–357.
- Hamilton, R. L. (2000) *Brain Pathol.* 10, 378–384.
- Arai, H., Lee, V. M.-Y., Messinger, M. L., Greenberg, B. D., Lowery, D. E. & Trojanowski, J. Q. (1991) *Ann. Neurol.* 30, 686–693.
- Van Gool, D., De Strooper, B., Van Leuven, F. & Dom, R. (1995) *Dementia* 6, 63–68.
- Halliday, G., Brooks, W., Arthur, H., Creasey, H. & Broe, G. A. (1997) *Neurosci. Lett.* 227, 49–52.
- Hsia, A., Masliah, E., McConlogue, L., Yu, G., Tatsuno, G., Hu, K., Kholodenko, D., Malenka, R. C., Nicoll, R. A. & Mucke, L. (1999) *Proc. Natl. Acad. Sci. USA* 96, 3228–3233.
- Klein, W. L., Krafft, G. A. & Finch, C. E. (2001) *Trends Neurosci.* 24, 219–224.
- Rochet, J. C., Conway, K. A. & Lansbury, P. T., Jr. (2000) *Biochemistry* 39, 10619–10626.
- Lewis, J., Dickson, D. W., Lin, W. L., Chisholm, L., Corral, A., Jones, G., Yen, S. H., Sahara, N., Skipper, L., Yager, D., et al. (2001) *Science* 293, 1487–1491.
- Gotz, J., Chen, F., van Dorpe, J. & Nitsch, R. M. (2001) *Science* 293, 1491–1494.

## NEW EMBO MEMBER'S REVIEW

## From Alzheimer to Huntington: why is a structural understanding so difficult?

Piero Andrea Temussi<sup>1,2</sup>, Laura Masino and Annalisa Pastore<sup>2</sup>National Institute for Medical Research, Medical Research Council, The Ridgeway, Mill Hill, London NW7 1AA, UK and <sup>1</sup>Department of Chemistry, University of Naples 'Federico II', Via Cinthia 45, I 80126 Naples, Italy<sup>2</sup>Corresponding authors

e-mail: pat@chemistry.unina.it or apastor@nimr.mrc.ac.uk

An increasing family of neurodegenerative disorders such as Alzheimer's, Parkinson's and Huntington's diseases, prion encephalopathies and cystic fibrosis is associated with aggregation of misfolded polypeptide chains which are toxic to the cell. Knowledge of the three-dimensional structure of the proteins implicated is essential for understanding why and how endogenous proteins may adopt a non-native fold. Yet, structural work has been hampered by the difficulty of handling proteins insoluble or prone to aggregation, and at the same time that is why it is interesting to study these molecules. In this review, we compare the structural knowledge accumulated for two paradigmatic misfolding disorders, Alzheimer's disease (AD) and the family of poly-glutamine diseases (poly-Q) and discuss some of the hypotheses suggested for explaining aggregate formation. While a common mechanism between these pathologies remains to be proven, a direct comparison may help in designing new strategies for approaching their study.

**Keywords:** aggregation/amyloid/misfolding/poly-glutamine/structure

## Misfolded proteins: the cause of a new family of diseases

We are accustomed to regarding genetic diseases as linked to the loss of function of one or more gene products. However, the 'one gene, one protein, one function' hypothesis has by now been contradicted more often than confirmed. One of the most interesting examples in which this concept seems to fail is represented by an increasing family of neurodegenerative disorders such as Alzheimer's, Parkinson's and Huntington's diseases, prion encephalopathies and cystic fibrosis (Taylor *et al.*, 2002). The hallmark of these otherwise unrelated diseases is the formation of aggregates containing misfolded proteins, i.e. proteins in a non-native folding state, with a concomitant gain of function which eventually leads to neuronal death. Gain of function rather than loss of function is supported by the observation that the aggregates are toxic *per se* (Spillantini *et al.*, 1998; Hardy and Selkoe, 2002). The aggregates have various supramolecular organizations and, in most cases, form structurally well-defined

insoluble fibrillar deposits called amyloids (Glenner and Wong, 1984). In one case (prion diseases) aggregates are even believed to be responsible for disease transmission (Prusiner, 1995). What are the structural mechanisms that lead to aggregate formation of endogenous proteins? What makes the aggregates toxic? A great deal of literature has appeared in the last decade to address these questions. Since all members of the family of diseases are linked to a mechanism of aberrant protein folding, knowledge of the three-dimensional structure of the proteins implicated, both in their 'healthy' and in their pathological forms, is the prerequisite for understanding the mechanism of aggregate formation and, eventually, preventing it. Yet, only relatively limited structural information is currently available. Some of the structural hypotheses formulated to explain aggregate formation and toxicity have migrated from one field to the other, suggesting, at least apparently, the possibility of a somewhat similar mechanism. It is however important to question closely whether such a common mechanism exists or if the analogies are only apparent. Here we review in parallel some of the structural hypotheses currently suggested for two disease families, Alzheimer's disease (AD) (and related tauopathies) and the family of poly-glutamine (poly-Q) diseases, selected as paradigms of misfolding disorders (Table I). A direct comparison which analyses commonalities and differences among them may be helpful for increasing our understanding of misfolding diseases.

## A supramolecular view: fibres and aggregates

The first observation of brain aggregates was carried out by Alois Alzheimer, a German physician who, in 1906, presented a case history of a patient affected by a then unknown brain disorder (Kraepelin, 1910). The autopsy of the patient's brain showed the presence of two distinct types of lesions: extracellular deposits forming plaques and intracellular bundles of neurofibrillary tangles (NFTs). These lesions are now considered the invariant pathological feature of AD (for a recent review see Hardy and Selkoe, 2002). The current dominant view is that the plaques deposited outside and around the neurons are intrinsically toxic (Hardy and Selkoe, 2002), although more recent findings suggest the possibility that the intraneuronal deposits are the direct cause of toxicity (Mochizuki *et al.*, 2000; Kienlen-Campard *et al.*, 2002). According to the so-called amyloid hypothesis, tangles are considered only a secondary event as far as the time sequence in the disease progression is concerned, being a consequence of the formation of amyloid  $\beta$  (A $\beta$ ) plaques (Hardy and Selkoe, 2002). When brain lesions are made up only of intracellular bundles of self-assembled tau proteins, without accumulation of A $\beta$  in plaques, the

**Table I.** Summary of main diseases discussed in the review

Disease family	Diseases	Responsible proteins	Aggregates (localization)	Reference
Alzheimer's (AD)		amyloid precursor protein (APP)	plaques of fibrils (extracellular)	Hardy and Selkoe, (2002)
Tauopathies <sup>a</sup>	Amyotrophic lateral sclerosis/Parkinsonism-dementia complex Argyrophilic grain dementia Corticobasal degeneration Dementia pugilistica Diffuse neurofibrillary tangles with calcification Frontotemporal dementia with Parkinsonism linked to chromosome 17 Pick's disease Progressive subcortical gliosis Progressive supranuclear palsy Tangle only dementia	tau protein	neurofibrillary tangles (intracellular)	Lee <i>et al.</i> , (2001)
Poly-Q	Huntington's (HD) Spinobulbar muscular atrophy (Kennedy disease or SBMA) Dentatorubral-pallidoluysian atrophy (Haw-River syndrome or DRPLA) Spinocerebellar ataxia 1 (SCA1) Spinocerebellar ataxia 2 (SCA2) Spinocerebellar ataxia 3 (Machado-Joseph or SCA3) Spinocerebellar ataxia 6 (SCA6) Spinocerebellar ataxia 7 (SCA7)	Huntingtin  androgen receptor  atrophin-1 ataxin-1 ataxin-2  ataxin-3 VDCC ataxin-7	amorphous or amyloid-like (intracellular) <sup>b</sup>	Masino and Pastore, (2002)

<sup>a</sup>Pathologies, other than AD, in which tau-positive neurofibrils are the predominant neuropathologic feature.

<sup>b</sup>In SCA6 nuclear aggregates are accompanied by cytoplasmic aggregates which are predominant.

diseases are usually distinct from AD and called tauopathies (Lee *et al.*, 2001). NFTs are nevertheless as toxic as amyloid plaques and in tauopathies lead to clinical symptoms similar to those of AD (Spillantini *et al.*, 1998).

The poly-Q disorders [which include Huntington's chorea, spinobulbar muscular atrophy (SBMA), dentatorubral-pallidoluysian atrophy and spinocerebellar ataxias (SCAs)] are also associated with the formation of neuronal nuclear inclusions (NI) (Mangiarini *et al.*, 1996). In several cases, NI are spherical aggregates, sometimes assembled by insoluble amyloid-like fibrils (Scherzinger *et al.*, 1999; McGowan *et al.*, 2000). Aggregates outside the nucleus have also been observed, but it has been shown recently that nuclear localization is required for toxicity (Yang *et al.*, 2002).

The pathologies of AD and poly-Q diseases are distinct, but both involve aggregate formation and degeneration of a specific subset of neuronal cells. The two disease families could therefore share a common mechanism of pathogenesis, in which the aggregates affect the cellular functions and eventually cause neuronal death.

A causative link between aggregation and disease is not however universally acknowledged. It has been conversely suggested that the aggregates could have a protective role for neuronal cells, being the result of the cell's attempts to proteolytically degrade or inactivate the toxic expanded protein (Zoghbi and Orr, 2000; Hardy and Selkoe, 2002). Pathogenesis could thus be initiated by other causes and only result in amyloid fibre formation.

## A molecular view: proteins or peptides?

While predisposition to AD has been linked to mutations of several genes, including those of presenilins and apolipoprotein E, mainly two protein components are present in the two types of AD aggregates (reviewed in Hardy and Selkoe, 2002). Plaques are generated by deposition of the amyloid peptides (A $\beta$ ), which are degradation products of the amyloid precursor protein (APP). APP is a transmembrane cell surface glycoprotein, expressed in five isoforms, with APP(695) being the dominant isoform in brain. APP can be cleaved by three different proteases, called  $\alpha$ ,  $\beta$  and  $\gamma$  secretases. When APP is concomitantly hydrolysed by  $\beta$ -secretase at the N-terminus of A $\beta$  and by the  $\gamma$ -secretase within the membrane (Lichtenthaler *et al.*, 2002), the two main products, A $\beta$ (1–40) and A $\beta$ (1–42), migrate outside the cell and give rise to fibrils. When APP is cut by  $\alpha$ -secretase, the resulting soluble peptides are generally considered non-toxic, although a recent report shows that the p3 peptide derived by  $\alpha$ - and  $\gamma$ -secretase cleavage of APP is also toxic (Wei *et al.*, 2002). A $\beta$ (1–42) readily aggregates and seeds the formation of fibrils that can then act as templates for plaque formation. Several shorter synthetic peptides corresponding to partial sequences of A $\beta$ (1–42) are able to form fibrils *in vitro* and have been studied along with 'natural' A $\beta$ .

NFTs are mostly composed of the tau protein (from which tauopathies are named) (Garcia and Cleveland,

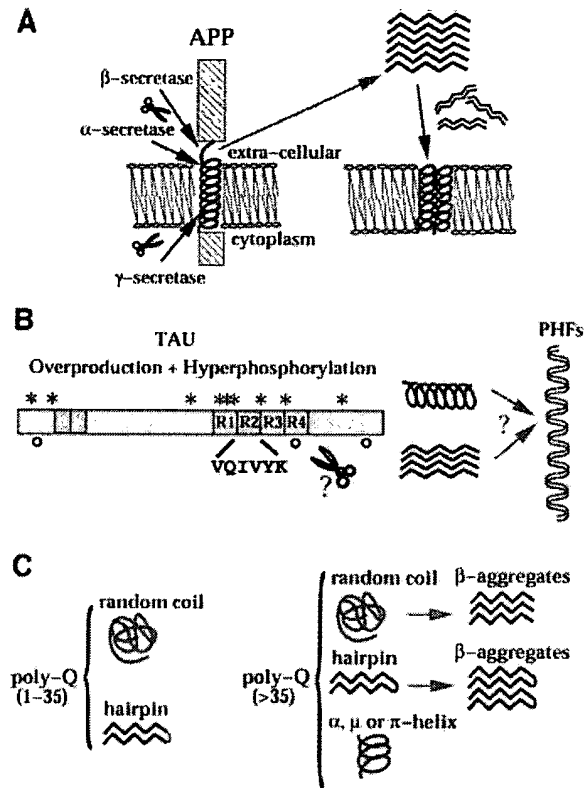


**Fig. 1.** Hypothetical mechanisms of conformational transitions for A $\beta$  peptides (A), tau (B) and poly-Q containing proteins (C). (A) The peptides are proteolytically cleaved from APP, precipitate as  $\beta$ -structures in equilibrium with oligomers which may eventually redissolve into the membrane. The lipid double layer is shown schematically in green. (B) A schematic picture of the architecture of tau. The four repeats are indicated with R1–R4. Regions differentially spliced are coloured in green. The sites identified as calpain and caspase-3 cleavage are indicated with stars and open circles respectively (Canu *et al.*, 1998). The proteolytic products may assemble or nucleate aggregate formation (PHFs). (C) Summary of the current models of conformational transitions involving poly-Q tracts both in the pathological and non-pathological range. For a more detailed account see Masino and Pastore (2002).

2001; Hardy and Selkoe, 2002), a highly hydrophilic microtubule-associated protein whose main function is microtubule stabilization, but also covers membrane interactions and anchoring of enzymes (Brandt *et al.*, 1995; Sontag *et al.*, 1999). Tangle formation is accompanied by further increase of tau production, hyperphosphorylation and loss of microtubule binding in the affected neurons. Proteolysis has been proposed to be important also for tau since the C-terminus of tau, when cleaved by proteases, generates cytotoxic fragments (Canu *et al.*, 1998). These and other fragments are thought to nucleate tangle formation from full-length tau (von Bergen *et al.*, 2000). However, it remains much more uncertain than for the well-defined A $\beta$  which regions of tau are responsible for tangle formation.

Poly-Q diseases result from expansion of CAG nucleotide repeats that encode poly-Q tracts within the corresponding gene product (reviewed in Paulson, 1999; Zoghbi and Orr, 2000). The resulting proteins show no sequence homology outside the poly-Q, span different lengths, have

different cellular localization and, when known, different functions. The only common feature is the presence of poly-Q tracts, which are, however, located in different regions of the corresponding proteins. A direct role of poly-Q in neurotoxicity has been demonstrated (Ordway *et al.*, 1997; Yang *et al.*, 2002). Interestingly, pathological effects occur in patients only when the length of poly-Q exceeds a rather sharp threshold of 35–40 glutamines. The length of the poly-Q tract correlates directly with the age of onset and with the severity of the symptoms in the diseases. The molecular composition of NI is much more heterogeneous than that of the AD aggregates, since they contain the ubiquitinated affected protein, proteolytic fragments, chaperones and other poly-Q proteins. While for AD and related tauopathies the mechanism of aggregation is now widely accepted to be linked to proteolysis of APP (Hardy and Selkoe, 2002) and tau (von Bergen *et al.*, 2000), it is still unclear whether proteolysis is a universal event also for poly-Q proteins: proteolytic fragments and not the full-length proteins have been observed in NI for at least three poly-Q diseases (huntingtin, the androgen receptor and ataxin 1) (DiFiglia *et al.*, 1997; Wellington *et al.*, 1998; Welch and Diamond, 2001; Lunkes *et al.*, 2002). Huntingtin exon 1 with an expanded poly-Q is sufficient to cause a progressive neurological phenotype in transgenic mice (Mangiarini *et al.*, 1996). However, other reports suggest that the expanded proteins are more protease resistant and that release of N-terminal fragments of huntingtin occurs also in the non-toxic non-expanded protein (Dyer and McMurray, 2001; Kim *et al.*, 2001; Lunkes *et al.*, 2002).

Clarification of the precise nature of the aggregates obviously bears important consequences for structural/functional studies of tau and poly-Q proteins.

### Structural hypotheses on conformational transitions: how to solubilize the 'insoluble'

The prevailing hypothesis for explaining aggregation and amyloid formation involves a structural transition of a polypeptide chain from a native fold to an improperly folded or misfolded conformation. Much attention has been paid to understanding the molecular mechanisms producing this transition. The starting point for these studies implies the characterization of the structure of the non-aggregated protein or protein fragments. These are often referred to as the 'soluble form', as opposed to aggregates, but the actual situation is more complex since the starting conformation may not necessarily be soluble, especially at concentrations suitable for structural studies, as in the case of A $\beta$ . Structural studies are therefore strongly hampered by the low solubility in water and by the tendency of the proteins and peptides to aggregate, i.e. ironically for the very reason why it is interesting to study them. Several strategies have been devised to overcome these limitations.

In AD, A $\beta$  are believed to exist in an  $\alpha$ -helical conformation when it is part of the transmembrane APP (Ortega-Aznar *et al.*, 2000), with an amphipathic character distributed along the sequence: the hydrophilic N-terminus of the A $\beta$  is exposed to an aqueous environment whereas the highly hydrophobic C-terminus is embedded in the membrane lipids (Figure 1A). To overcome their lack of

solubility and to mimic the membrane environment, most solution studies of A $\beta$  have been performed either in mixtures of water and alcohols or in micellar solutions (Serpell, 2000; and references therein). In all these media, A $\beta$  assume helical conformations, characterized by two helical segments interrupted by a central tract that was termed the 'kink region' (Coles *et al.*, 1998; Shao *et al.*, 1999). However, the length of the helical segments and the conformation of the kink region varies according to the media employed. In the structure of A $\beta$ (1–40) in a trifluoroethanol (TFE)/water mixture (Sticht *et al.*, 1995) the two helices, spanning residues 15–23 and 31–35, are separated by a disordered region. In a mixture of hexafluoroisopropanol and water the kink region of A $\beta$ (1–42) has been found to adopt a regular type I  $\beta$ -turn, yielding a well-defined tertiary structure (Crescenzi *et al.*, 2002). The striking similarity of this structure with that of the fusion domain of haemagglutinin of influenza virus hints to a possible mechanism of toxicity of A $\beta$  (discussed later). A random coil conformation has instead been observed in aqueous solution for Met-oxidized A $\beta$ (1–40) and smaller fragments (Jarvet *et al.*, 2000; Zhang *et al.*, 2000; Riek *et al.*, 2001) and in dimethylsulfoxide and water mixtures (Crescenzi *et al.*, 2002).

Sequence analysis of tau suggests that it is a natively unfolded protein with an even distribution of hydrophobic fragments along its sequence and up to four repeats of ~30 residues in its central region (Ruben *et al.*, 1991; von Bergen *et al.*, 2000) (Figure 1B). Experimental information derived from electron microscopy (EM), small angle X-ray scattering and NMR of tau confirms that the protein is essentially unfolded with little  $\alpha$ -helix and  $\beta$ -sheet content (Crowther and Wischik, 1985; Kirschner *et al.*, 1986; Schweers *et al.*, 1994). Peptides from tau are much more soluble than A $\beta$ , making solution studies less problematic. Short synthetic peptides spanning tau repeat sequences are mostly random in solution but were shown to be able to aggregate as  $\beta$ -structures (von Bergen *et al.*, 2000). A peptide from the C-terminus (residues 423–441), which forms an alternative nucleation region of NFTs, forms a regular helix in a TFE/water mixture with a helical stabilizing C-capping motif (Esposito *et al.*, 2000).

More debated is the nature of the conformation and the structural transition of poly-Q, for which experimental validation is even harder. In addition to the solubility problems, it is hard to produce this homopolymer both by conventional peptide synthesis and by recombinant methods. In 1993, Perutz proposed that poly-Q chains could form antiparallel  $\beta$ -strands held together by hydrogen bonds between side chain and main chain amides (Perutz *et al.*, 1993). These 'polar zippers' would pair either intramolecularly (leading to a  $\beta$ -hairpin) or intermolecularly (leading to aggregates) when the poly-Q length exceeded a threshold. Although since then this hypothesis has strongly dominated the field, other researchers have invoked different models which imply transitions from random and  $\alpha$ -to- $\beta$  conformations (Lathrop *et al.*, 1998; Starikov *et al.*, 1999) (Figure 1C). In addition, an entirely different conformation, a right-handed helix with 6.2 residues/turn called  $\mu$ -helix, was suggested by Monoi (1995). Such structure has a cylindrical pore along its helical axis larger than in an  $\alpha$ -helix (~6.6 Å) and might be favoured in poly-Q sequences

owing to the unique possibility of hydrogen bonds involving the amide groups of glutamine side chains. Experimental evidence is mostly based on model peptide studies of poly-Q tracts, which have been solubilized using either hydrophilic flanking sequences or various mixtures of organic solvents, and on poly-Q sequences fused to different protein carriers (reviewed in Masino and Pastore, 2002). Attempts to characterize poly-Q structure in protein contexts different from the natural ones are justified by the observation that poly-Q is toxic independently of the specific protein (Ordway *et al.*, 1997). Most peptide and protein studies seem to alternatively support one of these hypotheses: in one, soluble poly-Q is in random coil conformation, in the second, it forms  $\beta$ -structures. The apparent contradictions between these studies may be reconciled into a unifying picture by considering that the results are dominated by the strong aggregative tendency of poly-Q in water. Only when either the solvent composition, the flanking regions or the carrier protein are able to offset the insolubility of poly-Q, can this then adopt a random coil conformation. Since long poly-Q tracts have stronger tendency to aggregate, the competing effect of the environment will have a reduced effect.

### Structural models of aggregates: how to study the 'insoluble'

While the insolubility of the non-aggregated proteins hampers solution studies, a structural characterization of the aggregates is, if possible, even harder since it has to deal with their amorphous nature. These circumstances have so far prevented the determination of a consensus structure at atomic detail of any of the major aggregates. The consensus hypothesis is that amyloid fibres are constituted by  $\beta$ -sheet conformations. Increasing experimental evidence shows in fact that it is possible to induce  $\beta$ -sheet fibril formation in many proteins *in vitro* (reviewed in Dobson, 1999). Figure 2 shows a comparison of current models of amyloid fibres (Serpell, 2000; and references therein), NFTs (Moreno-Herrero *et al.*, 2001) and poly-Q aggregates (Perutz *et al.*, 2002). Direct evidence from solid state techniques, such as X-ray fibre diffraction, solid-state NMR, fourier transform-infrared and EM shows unequivocally that amyloid AD plaques are composed of long straight fibres of 6–12 nm in diameter with a basic  $\beta$ -sheet conformation in the fibrils (Sunde *et al.*, 1997). The main controversy is whether in amyloid fibrils the  $\beta$ -strands are parallel, as indicated by work with solid-state NMR and electron paramagnetic resonance (Balbach *et al.*, 2002; Torok *et al.*, 2002) or antiparallel, as suggested by several X-ray diffraction studies (Serpell, 2000).

A water-filled nanotube structure formed by a single cylindrical  $\beta$ -sheet stabilized by backbone and side chain hydrogen bonds was suggested as a possible model for poly-Q fibres (Perutz *et al.*, 2002). No atomic model is yet available for NFTs. Morphological studies based on EM and atomic force microscopy show tangles as formed by intra-cellular paired helical filaments (PHF), which are assembled into two twisted ribbons with a helical pitch of ~75–80 nm (Crowther and Wischik, 1985; Pollanen *et al.*, 1997; Moreno-Herrero *et al.*, 2001). Conflicting evidence exists about the structural nature of PHF. A hexapeptide

306VQIVYK<sup>311</sup> from the beginning of the third repeat of tau has been shown to assemble into thin  $\beta$ -filaments (although without PHF appearance) and to nucleate PHFs from full-length tau (von Bergen *et al.*, 2000). Such results are, however, at variance with a preliminary report claiming a helical structure for unpurified PHFs isolated from brain samples of AD patients (Sadqi *et al.*, 2002).

### Why should aggregates be toxic?

Even when we understand the mechanism leading to aggregate formation, we shall still need to explain how and why these are toxic for the cell. It is hard to imagine how a common mechanism could be consistent with the very different localizations of the polypeptide chains involved in AD and poly-Q diseases. Toxicity is particularly obscure for AD where, if toxicity were due to the plaques external to the neurons, aggregates could not interfere directly with the cell metabolism. It is natural to think that plaques adjacent to the cellular membrane can directly damage it. Whereas a trivial explanation might suggest the mechanical blockage by plaques of all cellular exchanges with the outer environment, a widely invoked cause of membrane damage has been free radical oxidative stress (Varadarajan *et al.*, 2000). On a more general level, the idea that amyloid plaques in AD act as large reservoirs of species in equilibrium with smaller neurotoxic oligomers is gaining more credit (Walsh *et al.*, 2002).

A specific mechanism for the toxicity of oligomeric assemblies seems to be suggested by solution studies of isolated A $\beta$ : the surprising similarity of the structure of A $\beta$ (1–42) to the fusion domain of influenza haemagglutinin in an apolar microenvironment (Crescenzi *et al.*, 2002) points to membrane poration as the key event for the peptide neurotoxicity. The  $\alpha$ -helical peptide would induce formation of membrane channels, allowing the penetration of substances (such as metal ions) that can cause neuronal death (Rhee *et al.*, 1998; Lin *et al.*, 2001). The ability of A $\beta$  to induce vesicle fusion (Pillot *et al.*, 1996) and the recent observation that A $\beta$  can enhance infection at the stage of attachment or entry into the cell of several viruses further support this hypothesis (Wojtowicz *et al.*, 2002).

A similar mechanism has been proposed to explain the toxicity of expanded poly-Q. Poly-Q stretches can induce large membrane-depolarizing ion channels in membranes which could damage the cell by altering the ionic balance (Hirakura *et al.*, 2000; Monoi *et al.*, 2000). The  $\mu$ -helix conformation (Monoi, 1995) would provide a justification for the puzzling threshold that separates pathological (>35–40) from non-pathological lengths of poly-Q tracts in poly-Q diseases. The minimum peptide length required for the  $\mu$ -helix to span the hydrophobic core of a lipid bilayer (estimated to be ~3 nm) is ~37 residues. Similarly, the restraints imposed by the helical nature of the model proposed by Perutz *et al.* (2002) impose a minimum of 40 residues for stabilizing the nanotube structure. The poration hypothesis is however not supported by a membrane localization of most of poly-Q proteins, in conflict with the possibility of a common mechanism related to poly-Q. Alternative albeit only theoretical models relate the threshold to an intrinsic random coil instability with respect to  $\beta$ -conformations in chains containing >40 glutamines (Starikov *et al.*, 1999). A

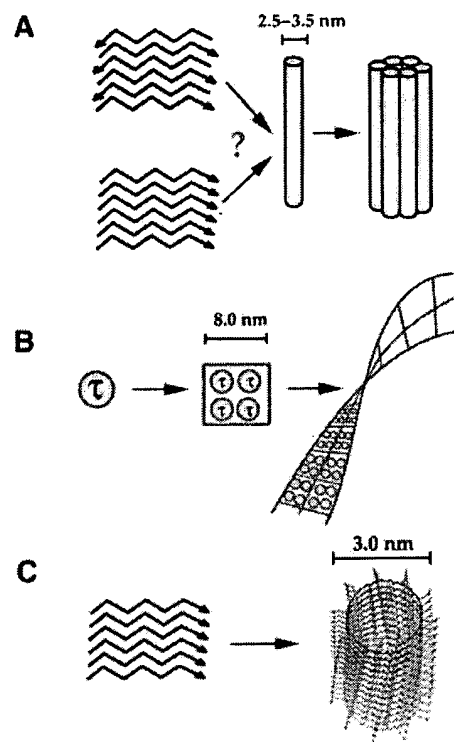


**Fig. 2.** Comparison of current models of amyloid fibres (A), tangles (B) and poly-Q aggregates (C). (A) The amyloid protofilament of 2.5–3.5 nm diameter would originate from  $\beta$ -strands running perpendicular to the fibre axes, although it is still disputed whether they run parallel or anti-parallel (Serpell, 2000). Several protofilaments are thought to further assemble to form mature fibrils. (B) Although no details are available yet about the molecular arrangement of tau in tangles, ample evidence of their morphology suggests an arrangement of paired helical filaments (Moreno-Herrero *et al.*, 2001). (C) Model of water-filled nanotube in which the poly-Q forms a helical fibre with 20 residues per turn (Perutz *et al.*, 2002). The main chains are shown in purple. The side chains (shown in green) protrude inside and outside the cylinder surface, according to  $\beta$ -sheet periodicity. Hydrogen bonds are formed both between the main chains and the side chains and would stabilize the structure.

structural difference could promote interactions with cellular components which do not recognize short poly-Q proteins and/or lead more readily to aggregates. In both cases, the normal cellular functions would be altered.

### Towards a unifying picture?

Although AD and poly-Q proteins were identified 10–15 years ago, still relatively few structural studies describe the conformation of these proteins both in their pathological and non-pathological forms. This is at least partially due to the specific challenges posed by this unusual class of polypeptides which respond differently to different environments. In all cases, significant information can be obtained only by using a multidisciplinary approach in which the properties in solution and in a solid-state environment are compared. While a common mechanism for misfolding diseases still remains to be proven, a unifying picture emerging from the current studies is that all peptides generated by proteolysis of the parent proteins

are water insoluble and aggregate *in vitro*. However, protein fusion, complexation or a solvent medium can offset aggregation. It is clear that unambiguous identification of the entity prone to aggregation and a more detailed understanding of the structural bases of the conformational transition is a key step for designing possible therapies.

## Acknowledgements

We are indebted to Arthur M.Lesk for providing the coordinates of the water-filled nanotube model. We thank Salvatore Adinolfi, Barbara Bardoni and Enzo Lalli, for critical reading of the manuscript.

## References

- Balbach,J.J., Petkova,A.T., Oyler,N.A., Antzutkin,O.N., Gordon,D.J., Meredith,S.C. and Tycko,R. (2002) Supramolecular structure in full-length Alzheimer's  $\beta$ -amyloid fibrils: evidence for a parallel  $\beta$ -sheet organization from solid-state nuclear magnetic resonance. *Biophys. J.*, **83**, 1205–1216.
- Brandt,R., Leger,J. and Lee,G. (1995) Interaction of tau with the neural plasma membrane mediated by tau's amino-terminal projection domain. *J. Cell Biol.*, **13**, 1327–1340.
- Canu,N. *et al.* (1998) Tau cleavage and dephosphorylation in cerebellar granule neurons undergoing apoptosis. *J. Neurosci.*, **18**, 7061–7074.
- Coles,M., Bicknell,W., Watson,A.A., Fairlie,D.P. and Craik,D.J. (1998) Solution structure of amyloid  $\beta$ -peptide(1–40) in a water-micelle environment. Is the membrane-spanning domain where we think it is? *Biochemistry*, **37**, 11064–11077.
- Crescenzi,O., Tomaselli,S., Guerrini,R., Salvadori,S., D'Ursi,A., Temussi,P.A. and Picone,D. (2002) Solution structure of the Alzheimer amyloid  $\beta$ -peptide (1–42) in an apolar microenvironment. *Eur. J. Biochem.*, **269**, 5642–5648.
- Crowther,R.A. and Wischik,C.M. (1985) Image reconstruction of the Alzheimer paired helical filament. *EMBO J.*, **4**, 3661–3665.
- DiFiglia,M., Sapp,E., Chase,K.O., Davies,S.W., Bates,G.P., Vonsattel,J.P. and Aronin,N. (1997) Aggregation of huntingtin in neuronal intranuclear inclusions and dystrophic neurites in brain. *Science*, **277**, 1990–1993.
- Dobson,C.M. (1999) Protein misfolding, evolution and disease. *Trends Biochem. Sci.*, **24**, 329–332.
- Dyer,R.B. and McMurray,C.T. (2001) Mutant protein in Huntington disease is resistant to proteolysis in affected brain. *Nat. Genet.*, **29**, 270–278.
- Esposito,G., Viglino,P., Novak,M. and Cattaneo,A. (2000) The solution structure of the C-terminal segment of tau protein. *J. Pept. Sci.*, **6**, 550–559.
- Garcia,M.L. and Cleveland,D.W. (2001) Going new places using an old MAP: tau, microtubules and human neurodegenerative disease. *Curr. Opin. Cell Biol.*, **13**, 41–48.
- Glenner,G.G. and Wong,C.W. (1984) Alzheimer's disease and Down's syndrome: sharing of a unique cerebrovascular amyloid fibril protein. *Biochem. Biophys. Res. Commun.*, **120**, 885–890.
- Hardy,J. and Selkoe,D.J. (2002) The amyloid hypothesis of Alzheimer's disease: progress and problems on the road to therapeutics. *Science*, **297**, 353–356.
- Hirakura,Y., Azimov,R., Azimova,R. and Kagan,B.L. (2000) Polyglutamine-induced ion channels: a possible mechanism for the neurotoxicity of Huntington and other CAG repeat diseases. *J. Neurosci. Res.*, **60**, 490–494.
- Jarvet,J., Damberg,P., Bodell,K., Eriksson,L.E.G. and Gräslund,A. (2000) Reversible random coil-to-sheet transition and the early stage of aggregation of the A(12–28). *J. Am. Chem. Soc.*, **122**, 4261–4268.
- Kienlen-Campard,P., Miolet,S., Tasiaux,B. and Octave,J.N. (2002) Intracellular amyloid- $\beta$  1–42, but not extracellular soluble amyloid- $\beta$  peptides, induces neuronal apoptosis. *J. Biol. Chem.*, **277**, 15666–15670.
- Kim,Y.J., Yi,Y., Sapp,E., Wang,Y., Cuiffo,B., Kegel,K.B., Qin,Z.H., Aronin,N. and DiFiglia,M. (2001) Caspase 3-cleaved N-terminal fragments of wild-type and mutant huntingtin are present in normal and Huntington's disease brains, associate with membranes and undergo calpain-dependent proteolysis. *Proc. Natl Acad. Sci. USA*, **98**, 12784–12789.
- Kirschner,D.A., Abraham,C. and Selkoe,D.J. (1986) X-ray diffraction from intraneuronal paired helical filaments and extraneuronal amyloid fibers in Alzheimer disease indicates cross- $\beta$  conformation. *Proc. Natl Acad. Sci. USA*, **83**, 503–507.
- Kraepelin,E. (1910) *Psychiatrie: Ein Lehrbuch für Studierende und Ärzte*. Barth, Leipzig, Germany, pp. 593–632.
- Lathrop,R.H., Casale,M., Tobias,D.J., Marsh,J.L. and Thompson,L.M. (1998) Modeling protein homopolymeric repeats: possible polyglutamine structural motifs for Huntington's disease. *Proc. Int. Conf. Intell. Syst. Mol. Biol.*, **6**, 105–114.
- Lee,V.M., Goedert,M. and Trojanowski,J.Q. (2001) Neurodegenerative tauopathies. *Annu. Rev. Neurosci.*, **24**, 1121–1159.
- Lichtenthaler,S.F., Behr,D., Grimm,H.S., Wang,R., Shearman,M.S., Masters,C.L. and Beyreuther,K. (2002) The intramembrane cleavage site of the amyloid precursor protein depends on the length of its transmembrane domain. *Proc. Natl Acad. Sci. USA*, **99**, 1365–1370.
- Lin,H., Bhatia,R. and Lal,R. (2001) Amyloid  $\beta$  protein forms ion channels: implications for Alzheimer's disease pathophysiology. *FASEB J.*, **15**, 2433–2444.
- Lunkes,A., Lindenberg,K.S., Ben-Haiem,L., Weber,C., Devys,D., Landwehrmeyer,G.B., Mandel,J.L. and Trotter,Y. (2002) Proteases acting on mutant huntingtin generate cleaved products that differentially build up cytoplasmic and nuclear inclusions. *Mol. Cell*, **10**, 259–269.
- Mangiarini,L. *et al.* (1996) Exon 1 of the HD gene with an expanded CAG repeat is sufficient to cause a progressive neurological phenotype in transgenic mice. *Cell*, **87**, 493–506.
- Masino,L. and Pastore,A. (2002) Glutamine repeats: structural hypotheses and neurodegeneration. *Biochem. Soc. Trans.*, **30**, 548–551.
- McGowan,D.P., van Roon-Mom,W., Holloway,H., Bates,G.P., Mangiarini,L., Cooper,G.J., Faull,R.L. and Snell,R.G. (2000) Amyloid-like inclusions in Huntington's disease. *Neuroscience*, **100**, 677–680.
- Mochizuki,A., Tamaoka,A., Shimohata,A., Komatsuzaki,Y. and Shoji,S. (2000) A $\beta$ 42-positive non-pyramidal neurons around amyloid plaques in Alzheimer's disease. *Lancet*, **355**, 42–43.
- Monoi,H. (1995) New tubular single-stranded helix of poly-L-amino acids suggested by molecular mechanics calculations. I. Homopolymer peptides in isolated environments. *Biophys. J.*, **69**, 1130–1141.
- Monoi,H., Futaki,S., Kugimiya,S., Minakata,H. and Yoshihara,K. (2000) Poly-L-glutamine forms cation channels: relevance to the pathogenesis of the polyglutamine diseases. *Biophys. J.*, **78**, 2892–2899.
- Moreno-Herrero,F., Valpuesta,J.M., Pérez,M., Colchero,J., Baró,A.M., Avila,J. and Montejo de Garcini,E. (2001) Characterization by atomic force microscopy and cryoelectron microscopy of tau polymers assembled in Alzheimer's disease. *J. Alzheimer's Dis.*, **3**, 443–451.
- Ordway,J.M. *et al.* (1997) Ectopically expressed CAG repeats cause intranuclear inclusions and a progressive late onset neurological phenotype in the mouse. *Cell*, **91**, 753–763.
- Ortega-Aznar,A., de la Torre,J. and Castelví,J. (2000) The CNS amyloid. *Rev. Neurol.*, **30**, 1175–1180.
- Paulson,H.L. (1999) Protein fate in neurodegenerative proteinopathies: polyglutamine diseases join the (mis)fold. *Am. J. Hum. Genet.*, **64**, 339–345.
- Perutz,M.F., Staden,R., Moens,L. and DeBaere,I. (1993) Polar zippers. *Curr. Biol.*, **3**, 249–253.
- Perutz,M.F., Finch,J.T., Berriman,J. and Lesk,A. (2002) Amyloid fibers are water-filled nanotubes. *Proc. Natl Acad. Sci. USA*, **99**, 5591–5595.
- Pillot,T., Goethals,M., Vanloo,B., Talussot,C., Brasseur,R., Vandekerckhove,J., Rosseneu,M. and Lins,L. (1996) Fusogenic properties of the C-terminal domain of the Alzheimer  $\beta$ -amyloid peptide. *J. Biol. Chem.*, **271**, 28757–28765.
- Pollanen,M.S., Markiewicz,P. and Goh,M.C. (1997) Paired helical filaments are twisted ribbons composed of two parallel and aligned components: image reconstruction and modeling of filament structure using atomic force microscopy. *J. Neuropathol. Exp. Neurol.*, **56**, 79–85.
- Prusiner,S.B. (1995) The prion diseases. *Sci. Am.*, **272**, 48–51, 54–57.
- Rhee,S.K., Quist,A.P. and Lal,R. (1998) Amyloid  $\beta$  protein-(1–42) forms calcium-permeable,  $Zn^{2+}$ -sensitive channel. *J. Biol. Chem.*, **273**, 13379–13382.
- Riek,R., Güntert,P., Döbel,H., Wipf,B. and Wüthrich,K. (2001) NMR studies in aqueous solution fail to identify significant conformational differences between the monomeric forms of two Alzheimer peptides



- with widely different plaque-competence, A  $\beta$ (1–40)(ox) and A  $\beta$ (1–42)(ox). *Eur. J. Biochem.*, **268**, 5930–5936.
- Ruben, G.C., Iqbal, K., Grundke-Iqbal, I., Wisniewski, H.M., Ciarrelli, T.L. and Johnson, J.E., Jr (1991) The microtubule-associated protein tau forms a triple-stranded left-hand helical polymer. *J. Biol. Chem.*, **266**, 22019–22027.
- Sadqi, M., Hernandez, F., Pan, U., Perez, M., Schaeberle, M.D., Avila, J. and Munoz, V. (2002)  $\alpha$ -helix structure in Alzheimer's disease aggregates of tau-protein. *Biochemistry*, **41**, 7150–7155.
- Scherzinger, E., Sittler, A., Schweiger, K., Heiser, V., Lurz, R., Hasenbank, R., Bates, G.P., Lehrach, H. and Wanker, E.E. (1999) Self-assembly of polyglutamine-containing huntingtin fragments into amyloid-like fibrils: implications for Huntington's disease pathology. *Proc. Natl Acad. Sci. USA*, **96**, 4604–4609.
- Schweers, O., Schonbrunn-Hanebeck, E., Marx, A. and Mandelkow, E. (1994) Structural studies of tau protein and Alzheimer paired helical filaments show no evidence for  $\beta$ -structure. *J. Biol. Chem.*, **269**, 24290–24297.
- Serpell, L.C. (2000) Alzheimer's amyloid fibrils: structure and assembly. *Biochim. Biophys. Acta*, **1502**, 16–30.
- Shao, H., Jao, S., Ma, K. and Zagorski, M.G. (1999) Solution structures of micelle-bound amyloid  $\beta$ -(1–40) and  $\beta$ -(1–42) peptides of Alzheimer's disease. *J. Mol. Biol.*, **285**, 755–773.
- Sontag, E., Nunbhakdi-Craig, V., Lee, G., Brandt, R., Kamibayashi, C., Kuret, J., White, C.L., III, Mumby, M.C. and Bloom, G.S. (1999) Molecular interactions among protein phosphatase 2A, tau and microtubules. Implications for the regulation of tau phosphorylation and the development of tauopathies. *J. Biol. Chem.*, **274**, 25490–25498.
- Spillantini, M.G., Bird, T.D. and Ghetti, B. (1998) Frontotemporal dementia and Parkinsonism linked to chromosome 17: a new group of tauopathies. *Brain. Pathol.*, **8**, 387–402.
- Starikov, E.B., Lehrach, H. and Wanker, E.E. (1999) Folding of oligoglutamines: a theoretical approach based upon thermodynamics and molecular mechanics. *J. Biomol. Struct. Dyn.*, **17**, 409–427.
- Sticht, H., Bayer, P., Willbold, D., Dames, S., Hilbich, C., Beyreuther, K., Frank, R.W. and Rosch, P. (1995) Structure of amyloid A4-(1–40)-peptide of Alzheimer's disease. *Eur. J. Biochem.*, **233**, 293–298.
- Sunde, M., Serpell, L.C., Bartlam, M., Fraser, P.E., Pepys, M.B. and Blake, C.C. (1997) Common core structure of amyloid fibrils by synchrotron X-ray diffraction. *J. Mol. Biol.*, **273**, 729–739.
- Taylor, J.P., Hardy, J. and Fischbeck, K.H. (2002) Toxic proteins in neurodegenerative disease. *Science*, **296**, 1991–1995.
- Torok, M., Milton, S., Kaye, R., Wu, P., McIntire, T., Glabe, C.C. and Langen, R. (2002) Structural and dynamic features of Alzheimer's A $\beta$  peptide in amyloid fibrils studied by site-directed spin labeling. *J. Biol. Chem.*, **277**, 40810–40815.
- Varadarajan, S., Yatin, S., Aksenova, M. and Butterfield, D.A. (2000) Review: Alzheimer's amyloid  $\beta$ -peptide-associated free radical oxidative stress and neurotoxicity. *J. Struct. Biol.*, **130**, 184–208.
- von Bergen, M., Friedhoff, P., Biernat, J., Heberle, J., Mandelkow, E.M. and Mandelkow, E. (2000) Assembly of tau protein into Alzheimer paired helical filaments depends on a local sequence motif ((306)VQIVYK(311)) forming  $\beta$  structure. *Proc. Natl Acad. Sci. USA*, **97**, 5129–5134.
- Walsh, D.M., Klyubin, I., Fadeeva, J.V., Cullen, W.K., Anwyl, R., Wolfe, M.S., Rowan, M.J. and Selkoe, D.J. (2002) Naturally secreted oligomers of amyloid  $\beta$  protein potently inhibit hippocampal long-term potentiation *in vivo*. *Nature*, **416**, 535–539.
- Wei, W., Norton, D.D., Wang, X. and Kusiak, J.W. (2002) A $\beta$  17–42 in Alzheimer's disease activates JNK and caspase-8 leading to neuronal apoptosis. *Brain*, **125**, 2036–2043.
- Welch, W.J. and Diamond, M.I. (2001) Glucocorticoid modulation of androgen receptor nuclear aggregation and cellular toxicity is associated with distinct forms of soluble expanded polyglutamine protein. *Hum. Mol. Genet.*, **10**, 3063–3074.
- Wellington, C.L. *et al.* (1998) Caspase cleavage of gene products associated with triplet expansion disorders generates truncated fragments containing the polyglutamine tract. *J. Biol. Chem.*, **273**, 9158–9167.
- Wojtowicz, W.M., Farzan, M., Joyal, J.L., Carter, K., Babcock, G.J., Israel, D.I., Sodroski, J. and Mirzabekov, T. (2002) Stimulation of enveloped virus infection by  $\beta$ -amyloid fibrils. *J. Biol. Chem.*, **277**, 35019–35024.
- Yang, W., Dunlap, J.R., Andrews, R.B. and Wetzel, R. (2002) Aggregated polyglutamine peptides delivered to nuclei are toxic to mammalian cells. *Hum. Mol. Genet.*, **11**, 2905–2917.
- Zhang, S. *et al.* (2000) The Alzheimer's peptide a  $\beta$  adopts a collapsed coil structure in water. *J. Struct. Biol.*, **130**, 130–141.
- Zoghbi, H.Y. and Orr, H.T. (2000) Glutamine repeats and neurodegeneration. *Annu. Rev. Neurosci.*, **23**, 217–247.

Received September 17, 2002; revised November 21, 2002;  
accepted November 28, 2002

# PEPTIDE AGGREGATION IN NEURODEGENERATIVE DISEASE

---

Regina M. Murphy

*Department of Chemical Engineering, University of Wisconsin, Madison,  
Wisconsin 53706; e-mail: murphy@che.wisc.edu*

**Key Words** amyloid, prion, beta-amyloid peptide, Huntington's disease,  
Alzheimer's disease

■ **Abstract** In the not-so-distant past, insoluble aggregated protein was considered as uninteresting and bothersome as yesterday's trash. More recently, protein aggregates have enjoyed considerable scientific interest, as it has become clear that these aggregates play key roles in many diseases. In this review, we focus attention on three polypeptides: beta-amyloid, prion, and huntingtin, which are linked to three feared neurodegenerative diseases: Alzheimer's, "mad cow," and Huntington's disease, respectively. These proteins lack any significant primary sequence homology, yet their aggregates possess very similar features, specifically, high  $\beta$ -sheet content, fibrillar morphology, relative insolubility, and protease resistance. Because the aggregates are noncrystalline, secrets of their structure at nanometer resolution are only slowly yielding to X-ray diffraction, solid-state NMR, and other techniques. Besides structure, the aggregates may possess similar pathways of assembly. Two alternative assembly pathways have been proposed: the nucleation-elongation and the template-assisted mode. These two modes may be complementary, not mutually exclusive. Strategies for interfering with aggregation, which may provide novel therapeutic approaches, are under development. The structural similarities between protein aggregates of dissimilar origin suggest that therapeutic strategies successful against one disease may have broad utility in others.

## CONTENTS

INTRODUCTION .....	156
SOLUTION STRUCTURES OF SELF-ASSEMBLING	
POLYPEPTIDES .....	158
A $\beta$ .....	159
PrP .....	160
Huntingtin .....	161
SOLID-STATE STRUCTURES OF SELF-ASSEMBLED	
POLYPEPTIDES .....	161
A $\beta$ .....	161
PrP .....	162

Huntingtin .....	163
KINETICS OF POLYPEPTIDE SELF-ASSEMBLY .....	163
ARE THE AGGREGATES TOXIC? .....	167
INHIBITORS OF AGGREGATION AND/OR TOXICITY .....	168
SUMMARY AND FUTURE DIRECTIONS .....	169

## INTRODUCTION

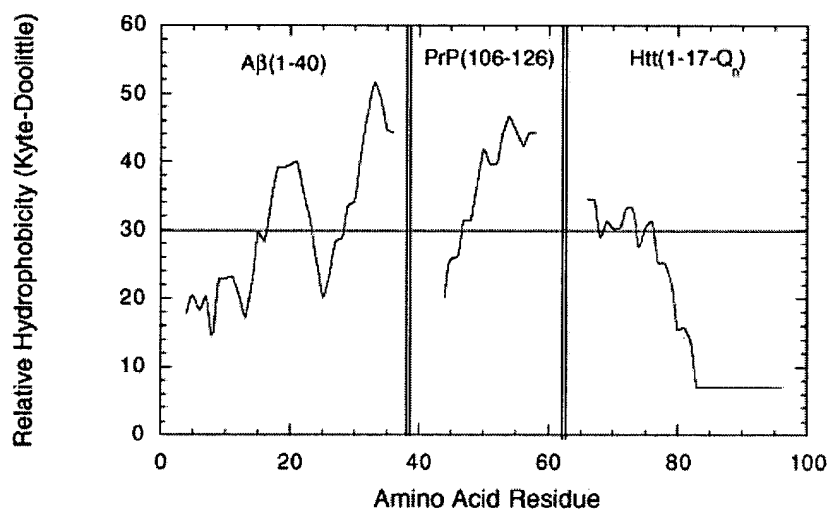
Amyloid is a general term describing protein aggregates with several physicochemical features in common: a fibrillar morphology, a predominantly  $\beta$ -sheet secondary structure, birefringence upon staining with the dye Congo red, insolubility in common solvents and detergents, and protease-resistance. Huntington's, Alzheimer's, and spongiform encephalopathy diseases are neurodegenerative disorders that have in common the presence of insoluble protein aggregates near the site of disease. Characteristic of Alzheimer's disease are senile plaques, extracellular deposits of beta-amyloid peptide fibrils surrounded by degenerating neurites. Spongiform encephalopathies include scrapie, "mad cow," and Creutzfeld-Jacob disease. Deposits of aggregated prion protein, some of which have the structural features of amyloid, are observed in brain tissues from humans and animals with these related diseases. Huntington's disease is characterized by insoluble aggregates of an N-terminal fragment of the protein huntingtin; these aggregates are intraneuronal inclusions localized to the nucleus. At least some of these huntingtin-containing nuclear inclusions stain with Congo red, and fibrillar structures have been observed, indicating that huntingtin aggregates may also be classified as amyloid-like (1).

None of the three polypeptides implicated in these diseases shares any primary sequence homology (Figure 1A), nor do they derive from similar sources. Beta-amyloid peptide ( $A\beta$ ) is a small ( $\sim 4$  kDa) proteolytic cleavage product of the  $\sim 70$ -kDa transmembrane protein APP (amyloid precursor protein) (2). Huntington's disease is causally linked to an expanded polyglutamine repeat domain ( $>35$  glutamines) in the N-terminal region of the huntingtin protein (htt). Huntingtin is a 350-kDa protein of unknown function localized in the cytoplasm; release of the N-terminal fragment by proteolytic cleavage seems to be required to initiate aggregation and transfer to the nucleus (3, 4). The prion protein (PrP) is a glycosylphosphatidylinositol-anchored glycoprotein ( $\sim 34$  kDa) that is a normal cell-surface component of neurons. No proteolysis or covalent modification appears to be required to initiate aggregation (5). Each aggregate has unique clinical manifestations, likely due to localized effects on specific subsets of neurons. Only the prion protein appears to be capable of transmitting disease.

Still, there are striking parallels (and differences) in the physicochemical properties of these three diverse polypeptides. Many detailed biophysical studies have been published, using both chemically synthesized peptides and recombinant proteins. Key experimental techniques include circular dichroism, FTIR, and NMR

**A.**

Protein fragment	Primary sequence (1-letter amino acid code) and predicted secondary sequence
A $\beta$ (1-40)	DAEFRHDSGYEVHHQKLVFFAEDVGSNKGAIIGLMVGGVV <div style="text-align: center;"> <span style="display: inline-block; width: 15%; border-top: 1px solid black; margin: 0 5px;"></span> <span style="display: inline-block; width: 15%; border-top: 1px solid black; margin: 0 5px;"></span> <span style="display: inline-block; width: 15%; border-top: 1px solid black; margin: 0 5px;"></span> <span style="display: inline-block; width: 15%; border-top: 1px solid black; margin: 0 5px;"></span> </div> <div style="text-align: center;"> <span style="display: inline-block; width: 15%; border-top: 1px solid black; margin: 0 5px;"></span> <span style="display: inline-block; width: 15%; border-top: 1px solid black; margin: 0 5px;"></span> <span style="display: inline-block; width: 15%; border-top: 1px solid black; margin: 0 5px;"></span> <span style="display: inline-block; width: 15%; border-top: 1px solid black; margin: 0 5px;"></span> </div> <div style="text-align: center;"> <span style="display: inline-block; width: 15%; border-top: 1px solid black; margin: 0 5px;"></span> <span style="display: inline-block; width: 15%; border-top: 1px solid black; margin: 0 5px;"></span> <span style="display: inline-block; width: 15%; border-top: 1px solid black; margin: 0 5px;"></span> <span style="display: inline-block; width: 15%; border-top: 1px solid black; margin: 0 5px;"></span> </div>
PrP(106-126)	KTNMHKHMAGAAAAGAVVGGLG <div style="text-align: center;"> <span style="display: inline-block; width: 10%; border-top: 1px solid black; margin: 0 5px;"></span> <span style="display: inline-block; width: 10%; border-top: 1px solid black; margin: 0 5px;"></span> <span style="display: inline-block; width: 10%; border-top: 1px solid black; margin: 0 5px;"></span> <span style="display: inline-block; width: 10%; border-top: 1px solid black; margin: 0 5px;"></span> </div> <div style="text-align: center;"> <span style="display: inline-block; width: 10%; border-top: 1px solid black; margin: 0 5px;"></span> <span style="display: inline-block; width: 10%; border-top: 1px solid black; margin: 0 5px;"></span> <span style="display: inline-block; width: 10%; border-top: 1px solid black; margin: 0 5px;"></span> <span style="display: inline-block; width: 10%; border-top: 1px solid black; margin: 0 5px;"></span> </div> <div style="text-align: center;"> <span style="display: inline-block; width: 10%; border-top: 1px solid black; margin: 0 5px;"></span> <span style="display: inline-block; width: 10%; border-top: 1px solid black; margin: 0 5px;"></span> <span style="display: inline-block; width: 10%; border-top: 1px solid black; margin: 0 5px;"></span> <span style="display: inline-block; width: 10%; border-top: 1px solid black; margin: 0 5px;"></span> </div>
Htt(1-17-Q <sub>n</sub> )	MATLEKLMKAFESLKSFQQQQQQQQQQQQQQQQQQQQ <div style="text-align: center;"> <span style="display: inline-block; width: 10%; border-top: 1px solid black; margin: 0 5px;"></span> <span style="display: inline-block; width: 10%; border-top: 1px solid black; margin: 0 5px;"></span> <span style="display: inline-block; width: 10%; border-top: 1px solid black; margin: 0 5px;"></span> </div> <div style="text-align: center;"> <span style="display: inline-block; width: 10%; border-top: 1px solid black; margin: 0 5px;"></span> <span style="display: inline-block; width: 10%; border-top: 1px solid black; margin: 0 5px;"></span> <span style="display: inline-block; width: 10%; border-top: 1px solid black; margin: 0 5px;"></span> </div> <div style="text-align: center;"> <span style="display: inline-block; width: 10%; border-top: 1px solid black; margin: 0 5px;"></span> <span style="display: inline-block; width: 10%; border-top: 1px solid black; margin: 0 5px;"></span> <span style="display: inline-block; width: 10%; border-top: 1px solid black; margin: 0 5px;"></span> </div>

**B.**

**Figure 1** Three aggregating polypeptides related to neurodegenerative disease. (A) Primary sequences of beta-amyloid A $\beta$ [1–40], human prion peptide PrP[106–126], and N-terminal huntingtin (htt) fragments. Primary sequences are taken from the Brookhaven Protein Data Bank. Full-length PrP and longer N-terminal huntingtin fragments are found in tissue deposits. The secondary structure predictions are based on a consensus of eight algorithms available in the Biology Workbench. Regions of disagreement between alternative algorithms are indicated as a choice of two structures. (B) Kyte-Doolittle hydropathy profiles. Residues below the dotted line are characterized as having hydrophilic side chains; residues above the dotted line are considered as having hydrophobic side chains.

spectroscopies; electron and atomic force microscopy; X-ray diffraction; analytical ultracentrifugation; size-exclusion chromatography; and light scattering. In this brief review, we discuss recent efforts (*a*) to elucidate the structure of these polypeptides in both soluble and aggregated states, (*b*) to define the kinetics of conversion of monomer to aggregate, and (*c*) to discover compounds capable of interfering with polypeptide aggregation. Such compounds may serve as leads in the effort to develop effective therapies against these devastating neurodegenerative diseases.

## SOLUTION STRUCTURES OF SELF-ASSEMBLING POLYPEPTIDES

An interesting hypothesis is that peptides prone toward amyloid fibril formation are those that as monomers fold into  $\alpha$ -helices in domains that are predicted to be  $\beta$ -sheet (6). To test this hypothesis against the three peptides under discussion, eight widely available secondary-structure prediction algorithms were used to analyze the peptide fragment sequences shown in Figure 1A. These algorithms were developed for globular soluble proteins, and their extension to the three polypeptides of interest here is problematic. With this caveat in mind, we report on the consensus sequence. All three peptides are predicted to have a disordered N-terminus. The C-terminus of A $\beta$ [1–40] (residues 1 through 40 of A $\beta$ ) is invariably predicted to be  $\beta$ -sheet, but the interior region (residues 11–21) is a domain of conformational confusion: The algorithms split about equally between helix or sheet. PrP[106–126] is predicted to contain an interior helix followed by a short  $\beta$ -strand. The huntingtin fragment is predicted to be primarily  $\alpha$ -helical. Based on these three peptide sequences, there is no consistent predicted propensity towards  $\beta$ -sheet, and hence, no support for the hypothesis. How well do these analyses compare to experimental data? The solution structures of monomeric polypeptides related to A $\beta$ , PrP, and htt have been reported by a number of investigators. A general feature is the conformational flexibility or adaptability of these polypeptides. In fact, proteins unrelated to known disease states can be induced to form amyloid fibrils by reducing the conformational stability of the folded globular protein (7). Perhaps a modified version of the hypothesis is more globally applicable; specifically, proteins and peptides prone to amyloid fibril formation are those that have a domain that readily adopts multiple conformations.

In Figure 1B we compare the hydrophobicity profiles of the three peptides, calculated using the Kyte-Doolittle method. The profiles of A $\beta$ [1–40] and PrP[106–126] are remarkably similar: Both are amphiphilic, with a hydrophilic N-terminus and hydrophobic C-terminus. The origins of these peptides have an impact on their hydrophobicity profile: Both A $\beta$  and the prion protein originate as membrane-embedded proteins. In fact, cleavage at the C-terminus of A $\beta$  occurs in the interior of the transmembrane domain. It is reasonable to hypothesize that their hydrophobic character plays a considerable role in the peptides' aggregation properties. Huntingtin is quite distinct. Full-length htt is cytoplasmic, not membrane derived

(although, interestingly, the aggregates are found not in the cytoplasm but in the nucleus). The polyglutamine expansion domain, strongly linked to aggregation and to disease, is quite hydrophilic on the Kyte-Doolittle scale. This analysis may be somewhat misleading; polyglutamine may act like a much more hydrophobic group due to strong hydrogen bonding between the polypeptide backbone and side chain amides. The distribution of hydrophobic side chains likely plays a significant role as well. It is possible to generate libraries of synthetic peptides of alternating polar and nonpolar residues that have a strong predilection towards self-associating into amyloid-like aggregates (8).

Several groups employed circular dichroism and NMR spectroscopies to explore solution-phase secondary structure of A $\beta$ -, PrP- and htt-related peptides. Results are summarized briefly in Table 1; each peptide is discussed in some detail in the following sections.

## A $\beta$

A $\beta$  undergoes substantial conformational shifts depending on its environment and can easily convert among disordered,  $\alpha$ -helical, and  $\beta$ -sheet conformers as solution conditions change. Under membrane-mimicking conditions, A $\beta$  contains a significant amount of  $\alpha$ -helical character (9–11). In physiological buffers, both random coil and  $\beta$ -sheet secondary structure are observed, with the  $\beta$ -sheet content increasing dramatically with peptide concentration (9). This indicates that the  $\beta$ -sheet-containing conformers are oligomeric. A $\beta$  conformation is both pH- and salt-sensitive, with an increase in  $\beta$ -sheet content in the presence of salt and in slightly acidic conditions. His residues at positions 12 and 13 likely contribute to the pH effect on the stability of aggregates, while the increase in  $\beta$ -sheet with salt likely derives from the peptide's hydrophobic regions (12, 13). NMR solution studies on A $\beta$ [10–35] indicated that the soluble monomer in water lacks regular secondary structural features (14). Rather, the peptide adopts a meta-stable collapsed coil structure around the central hydrophobic region (residues 17–21), with a large hydrophobic patch on the surface, and a turn in the 24–27 region (14).

**TABLE 1** Key secondary structural features of neurodegeneration-related aggregating peptides

	A $\beta$	PrP	htt
pH-dependence	$\beta$ -sheet $\uparrow$ with slightly acidic conditions	$\beta$ -sheet $\uparrow$ with slightly acidic conditions	—
Salt-dependence	$\beta$ -sheet $\uparrow$ with $\uparrow$ salt	$\beta$ -sheet $\uparrow$ with $\uparrow$ salt	—
Concentration-dependence	$\beta$ -sheet $\uparrow$ with $\uparrow$ concentration	$\beta$ -sheet $\uparrow$ with $\uparrow$ concentration	—
In membrane-mimicking solvents	$\alpha$ -helix	—	$\beta$ -sheet

A molecular dynamics study of A $\beta$ [10–35] noted structural fluctuations outside of the core hydrophobic (residues 17–21) domain and the turn (residues 24–27) region (15). The picture that emerges is of a peptide that adopts a helical structure when anchored in its natural membrane environment, that undergoes hydrophobic-driven collapse into a monomer lacking regular secondary structural features when released from the membrane by proteolysis, and that subsequently simultaneously oligomerizes and forms an extended  $\beta$ -sheet.

## PrP

The solution structure of PrP[106–126] in water is predominantly random coil with some  $\alpha$ -helical character (16), but reverts to  $\beta$ -sheet upon addition of a physiological concentration of salt (17). PrP fragments exhibit high conformational flexibility; addition of just five residues N-terminally to PrP[109–122] converts the stable conformer from  $\beta$ -sheet to  $\alpha$ -helix (18). The solution structure of full-length recombinant PrP has been determined by NMR. The N-terminus (residues 1–125, roughly half of the protein) has a long flexible tail; the C-terminal globular domain contains three  $\alpha$ -helices and a short anti-parallel  $\beta$ -sheet region (14, 19). Within the globular domain there is a flexible loop (residues 167–171) connecting the second  $\beta$ -strand and the second helix. C-terminal portions of helices 2 and 3 have relatively large conformational flexibility (14); indeed, synthetic peptides corresponding to these regions underwent time- and pH-dependent conversion to  $\beta$ -sheet aggregates (20). Under normal conditions, the solution structure of full-length PrP is quite stable; however, incubation of the protein under acidic conditions and in the presence of salt and low concentrations of denaturant causes a reproducible conversion to  $\beta$ -sheet oligomers (21). The His residue, lying between the hydrophilic N-terminus and hydrophobic C-terminus of PrP[106–126], may play a crucial role in the pH-dependence of aggregation and conformational change (22). Hydrogen exchange studies demonstrated that the conformational stability of the helical region of monomer PrP is not substantially different than other similar proteins (23). Removal of the single disulfide bond substantially reduces the stability of the helical monomer (24). Reduction of the disulfide bond, and acidic pH, caused a slow but reversible conformational shift in PrP[91–231] from helix to  $\beta$ -sheet; rather surprisingly, the  $\beta$ -sheet conformer was monomeric, stable, and completely soluble (25). Molecular dynamic simulations of PrP[121–231] (26) suggested formation of a hydrophobic cluster involving a short-lived addition of a third  $\beta$ -strand involving residues 123–125 to the antiparallel  $\beta$ -strands present in the stable folded prion monomer; perhaps this structural fluctuation initiates conversion from the predominantly helical monomer to the  $\beta$ -sheet aggregate (26). This picture is in agreement with the hypothesis, based on X-ray diffraction studies, that the central hydrophobic region of PrP forms a core that facilitates conversion of helical PrP to  $\beta$ -sheet (27). Taken together, these reports suggest that the native helical folded structure of monomeric PrP is only marginally stable, that short  $\beta$ -strands positioned near a hydrophobic core initiate conformation fluctuations, and that, by undergoing association, a  $\beta$ -sheet structure of greater stability can be obtained.

## Huntingtin

Very few detailed structural studies have been completed on polyglutamine or polyglutamine-containing htt fragments, in part because of difficulties in synthesis and insolubility. Based on circular dichroism studies, polyglutamines are strong  $\beta$ -sheet formers, retaining a  $\beta$ -sheet structure even in the helical-promoting solvent trifluoroethanol (28). The  $\beta$ -sheets are stabilized by hydrogen bonding between main-chain and side-chain amides. Indirect evidence suggested that long (40-mer) polyglutamine peptides can form stable  $\mu$ -helices, a novel tubular single-stranded helix with an inner wall containing a network of peptide backbone hydrogen bonds (29).

Thus, there are many parallels between PrP and A $\beta$  monomer structures in aqueous solution: significant regions of disorder and conformational flexibility, a hydrophobic cluster with  $\beta$ -sheet-forming tendencies, and His-mediated pH sensitivity. Full-length PrP is more stable as monomer than is A $\beta$ , likely because the former folds into a monomer with significant regular secondary structure whereas the latter does not. The difference is one of degrees, though, rather than of kind. Huntingtin, however, is a different kind of peptide. This was observed in the comparative analyses of the primary sequences (Figure 1A and 1B), and in the stability of the  $\beta$ -sheet in  $\alpha$ -helix promoting solvents (Table 1). Further structural studies of htt vis-a-vis A $\beta$  and PrP are needed to tease out a generalizable relationship between sequence, structure, and amyloidogenesis.

## SOLID-STATE STRUCTURES OF SELF-ASSEMBLED POLYPEPTIDES

Substantial conformational changes occur upon the conversion of soluble peptide to insoluble aggregate. Ascertaining the structure of the aggregates has proved to be a challenge. High resolution structural analysis of the aggregates has proven difficult to date because the fibrils are noncrystalline and do not provide clear NMR signals without special labeling techniques. Still, some advances have been made in ascertaining structure of the aggregates, especially for A $\beta$  aggregates. Useful techniques include electron and atomic force microscopy, X-ray diffraction, and solid-state NMR.

### A $\beta$

Long, semi-flexible, nonbranching fibrils of ~6–10 nm diameter are visible on electron microscope images of A $\beta$  aggregates. Cross-sectional analysis of electron microscope images of aggregated A $\beta$  (30) imputed a structural model of amyloid fibrils as an assembly of three to six laterally associated filaments. More detailed structural information was obtained in several studies employing atomic force microscopy. These studies yielded images of “protofilaments,” thin (3–4 nm) diameter nonbranching linear aggregates (31, 32). Growth of the filaments



proceeded bidirectionally (33). Protofilaments were indirectly observed by X-ray diffraction as well (34). These studies indicate that lateral association of several protofilaments produces the larger-diameter amyloid fibrils.

There are striking differences in conformation between A $\beta$  monomer and aggregate. In contrast to the conformational flexibility of the monomer, about half of the amide protons in multimeric A $\beta$  fibrils are highly-resistant to solvent exchange (35), indicating the core is highly stable. The central core region of A $\beta$  (residues 14–23) is competent to form fibrils, and deletion of this core from A $\beta$ [1–42] abrogates fibril formation (36). X-ray diffraction studies combined with molecular modeling produced a detailed structure of A $\beta$ [11–25] fibrils: a  $\beta$ -hairpin with a turn at residues 18–19, an antiparallel arrangement of  $\beta$ -strands perpendicular to the long axis of the fiber, forming continuous  $\beta$ -sheets, and inter-sheet interactions forming the filaments (37). These studies led to the proposal that A $\beta$  aggregates are composed of a highly-stable anti-parallel  $\beta$ -sheet core containing residues 14–23, with the hydrophobic C-terminus folding over this core. However, the applicability of this structural model to full-length A $\beta$  has been challenged by more recent solid-state NMR studies. A detailed examination of A $\beta$ [10–35] fibrils produced the surprising result that A $\beta$  forms parallel  $\beta$ -sheets, with no turns and with like residues in-register (38). Multiple-quantum solid-state NMR on full-length A $\beta$ [1–40] further supported a parallel, in-register arrangement of A $\beta$  monomers in the fibrils, with the parallel arrangement extending over at least four peptide chains (39).

## PrP

In vitro, many PrP fragments readily form amyloid-like aggregates. Electron micrograph images of PrP[106–126] and PrP[178–193] aggregates reveal the characteristic fibrillar nonbranching morphology of amyloid (20, 40). Similarly, PrP[90–231] can be induced, under partially denaturing conditions, to form both amorphous and fibrillar structures (21, 41). As observed in X-ray diffraction studies, PrP fragments with single-point mutations readily formed thin (4-nm diameter) fibrils with cross- $\beta$  sheet structure (27); hydrated wild-type fragments only infrequently folded into  $\beta$ -sheets. These authors proposed that the hydrophobic [106–126] domain serves as a core that facilitates conversion of the full-length PrP to  $\beta$ -sheet. This hypothesis is consistent with other reports showing that the hydrophobicity of the PrP fragment plays an important role in facilitating  $\beta$ -sheet formation and aggregation (42). In vitro, full-length PrP forms  $\beta$ -sheet aggregates after mild denaturation under slightly acidic conditions (21). Together, these studies indicate that PrP fragments form amyloid aggregates with physical properties very similar to those of A $\beta$ . The biological relevance of these in vitro studies has been questioned; in animals with scrapie, for example, amyloid aggregates are not always observed. This is in sharp contrast to the case with A $\beta$ , since the presence of A $\beta$  amyloid deposits is one of the defining features of Alzheimer's disease.

## Huntingtin

N-terminal huntingtin fragment htt(1-90) with 37 or more glutamines produced almost exclusively SDS-insoluble high-molecular-weight aggregates (43); by electron microscopy, aggregates had the classical fibrillar morphology, 100 to  $>1\ \mu\text{m}$  in length. Polyglutamines aggregate into semiflexible chains of 7–12-nm diameter; X-ray diffraction patterns are consistent with the cross- $\beta$  structure characteristic of amyloid fibrils (28). These reports demonstrate that peptides with long polyglutamine stretches can be induced to form amyloid aggregates *in vitro*. There remains a great deal to learn about the ultrastructure of htt aggregates. As with PrP, the biological relevance of *in vitro* htt amyloid aggregates has been questioned. There is limited evidence that the *in vivo* nuclear inclusions have amyloid-like properties (1).

## KINETICS OF POLYPEPTIDE SELF-ASSEMBLY

Elucidation of the kinetic pathway by which monomer is converted to fibril has occupied the attention of several research groups. Broadly speaking, there are two schools of thought: the nucleation-elongation model and the template-assisted model. In the nucleation-elongation model, initial self-assembly is slow and unfavorable until a critical size is reached. Once the “nucleus” is formed, further elongation by addition of monomers is rapid. In the template-assisted model, exposure of the monomer to an aggregate catalyzes a conformational change of the non- $\beta$  monomer into a  $\beta$ -rich form that is aggregation prone. Roughly equivalent to the nucleation-elongation versus template-assisted models, one can consider whether peptide self-assembly is spontaneous (does not require existence of pre-existing aggregate) or induced. Experimental and modeling efforts are briefly reviewed to see what evidence exists for either model of peptide assembly.

Spontaneous conversion of soluble  $A\beta$  monomer to amyloid is easily achieved in neutral or slightly acidic buffers containing physiologically relevant salt concentrations. Using turbidity to measure  $A\beta$  aggregation, Jarrett et al. (44) observed a concentration-dependent lag time in the appearance of aggregates and proposed a qualitative nucleation-elongation kinetic model for  $A\beta$  self-association. However, several other studies indicated that aggregates too small to be detectable by turbidity are present early in the aggregation process (45, 46). Thus, the lag phase observed in turbidity assays is likely not the time required for nucleation, but rather the time required for growth of sufficiently large aggregates. Lomakin et al. (47) employed dynamic light scattering to study fibril growth from  $A\beta$ [1–40] in 0.1 M HCl and proposed a detailed mathematical model based on these data along the lines of the nucleation-elongation hypothesis. Briefly, rapid reversible equilibration between monomers and micelles was postulated to occur, followed by spontaneous and irreversible generation of nuclei from micelles. Fibrils then grew by addition of monomer to the nucleus or fibril tip. A conceptually similar model was proposed by Inouye & Kirschner (48) in which association of multiple

monomers into a nucleus precedes indefinite reversible addition of monomers to polymer. This model was used to describe the pH-dependent growth of A $\beta$  aggregates, as monitored by Congo red binding. A detailed multi-step model of A $\beta$  aggregation kinetics was also proposed by Pallitto & Murphy (49); a schematic is shown in Figure 2. This pathway included: (a) rapid commitment to either stable monomer/dimer or unstable  $\beta$ -sheet intermediate, (b) cooperative association of intermediate into a multimeric "nucleus," (c) elongation of the "nucleus" into

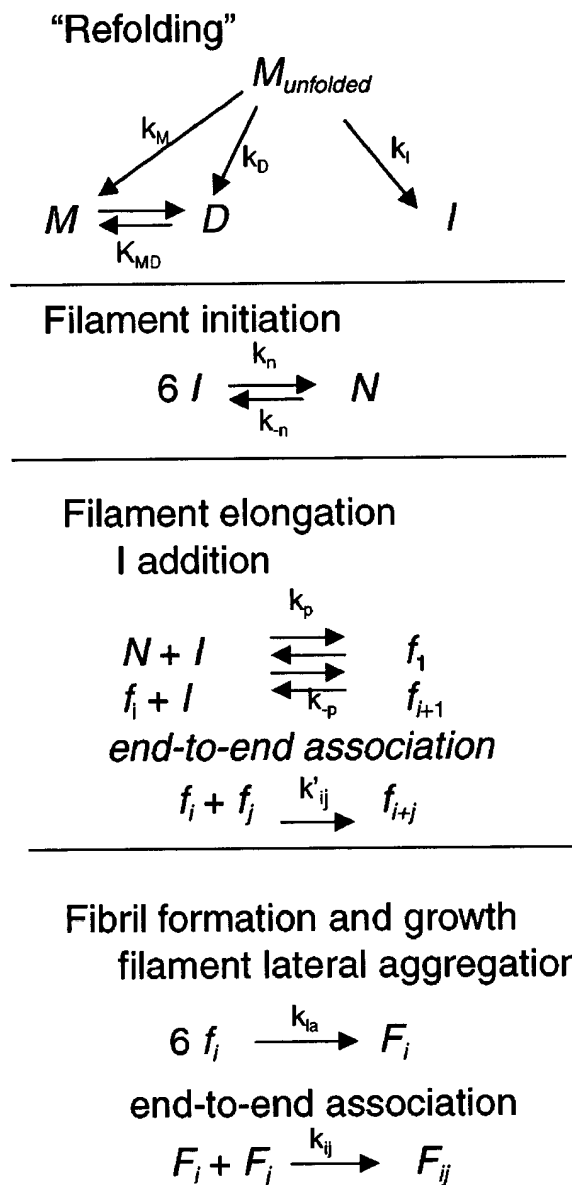


**Figure 2** Schematic of solution-phase self-association of A $\beta$ [1–40], adapted from (49). A mathematical model quantifying this schematic was derived and fitted using experimental data. Qualitatively similar pathways may be appropriate for aggregation of PrP and, possibly, htt.

filaments via addition of intermediate, (d) lateral aggregation of filaments into fibrils, and (e) fibril elongation via end-to-end association. The model was shown to be consistent with several sets of complementary experimental data (49). All of these models argue for the existence of a spontaneous mode of A $\beta$  self-assembly.

As mentioned above, PrP monomers are more stable than A $\beta$  in aqueous solution and conversion to aggregates is more difficult. Aggregation of PrP[106–126], as measured by turbidity, followed the classic sigmoidal curve observed with A $\beta$  (42). These data were interpreted as supportive of the nucleation-condensation model, but it could be that aggregates present during the early lag phase were not detectable by turbidity. Acidic pH and addition of low or moderate concentrations of a chemical denaturant were used to achieve conversion of the “native” structure of human recombinant PrP[90–231] (disordered N-terminus, helical C-terminus) to  $\beta$ -sheet. Conversion of PrP to  $\beta$ -sheet structure was invariably coincident with oligomerization (21, 24). Post et al. studied conformational changes and oligomerization with PrP[27–30] and PrP[90–231] solubilized with SDS. Once removed from the  $\alpha$ -helical stabilizing detergent solution, a rapid (<1 minute) conversion to  $\beta$ -sheet dimers was observed, followed by the appearance of larger oligomers after 20 minutes and the appearance of protease-resistant aggregates after several hours (50). Dimer to multimer conversion did not appear to require a cooperative step. Hydrogen-exchange studies demonstrated that conversion of helical PrP to  $\beta$ -sheet must proceed through a partially or completely unfolded intermediate (23). Urea-denatured PrP refolded to either its monomeric, predominantly helical form, or to its aggregation-prone, predominantly  $\beta$ -sheet form (41); the  $\alpha$ -helical form was kinetically favored, but the  $\beta$ -sheet form was thermodynamically more stable. The kinetics of refolding of the C-terminal region of PrP proceed at an extremely rapid pace (51), in further support of the hypothesis that PrP conversion does not occur through a populated folding intermediate state. Taken together, the data indicate that denatured PrP refolds into two alternative structures, one a stable folded helical monomer and the other an unstable aggregation-prone  $\beta$ -sheet-rich conformer. Although the quantitative details differ between the two peptides, the kinetic pathway shown in Figure 2, which was developed for A $\beta$ , captures the essential features of these data on PrP assembly.

Conversion of htt from monomer to aggregate depends strongly on the length of the polyglutamine domain. htt[1–90] with 32 or fewer glutamines was monomeric, but htt[1–90] with 37 or more glutamines produced almost exclusively SDS-insoluble high-molecular-weight aggregates with a fibrillar morphology (43). Using a turbidity assay, these researchers observed a lag-time in the onset of turbidity, with the length of the lag decreasing with increasing number of glutamines in the expansion region and increasing concentration. Addition of preformed fibrils eliminated the lag time (43). These studies led the authors to propose that htt aggregation proceeded via a nucleation-elongation mode. Due to the relative paucity of kinetic data on huntingtin aggregation, we cannot yet speculate whether htt association kinetics follow the pathway outlined in Figure 2. If the polyglutamine expansion domain is sufficiently long, the peptide can fold into a stable  $\beta$ -sheet monomer with

a hairpin turn (28). This result indicates that, unlike A $\beta$  or PrP, htt monomer with an expanded polyglutamine region may not require re-folding from the completely unfolded state to initiate slow aggregation.

A lattice-type model of protein folding and  $\beta$ -sheet propagation has been proposed and applied to the generation of PrP or A $\beta$  aggregates (52). Interesting conclusions from this study included (a) efficient propagation requires two opposite-facing binding sides, and (b) the most readily propagatable conformation is  $\beta$ -sheet rich. The hydrophobic nature of the peptides, or capacity for hydrogen bonding, was not explicitly considered. Perhaps any kind of oppositely faced attractive interaction can lead to propagation, which might explain why htt fragments, despite their hydrophilicity, can aggregate via backbone-side chain hydrogen bonding (28).

In the previous paragraphs, we discussed the kinetics of spontaneous conversion of solution-phase peptide to fibrillar aggregates. We now turn attention to induced conversion of solution-phase peptide to  $\beta$ -sheet aggregates. Roughly speaking, the difference between spontaneous and induced conversion parallels the difference between the nucleation-elongation and template-assisted models. Several lines of evidence indicate that template-assisted conversion is an important phenomenon in the peptide systems under discussion.

When pre-assembled A $\beta$  fibrils were immobilized onto a solid surface, monomeric, not oligomeric, A $\beta$  bound to the fibrils (53) via a “dock-lock” mechanism in which weak reversible binding of monomer to fibril was followed by a conformational change “locking” the monomer to the template (54). In a clever study, Esler et al. synthesized a highly constrained structural analog of soluble A $\beta$  and an analog that should more easily undergo conformational changes than wild-type A $\beta$ ; deposition rates were strongly dependent on conformational flexibility (55). These data support a template-assisted mechanism of growth, and suggest that the kinetic limit to deposition is the conformational transition of the soluble species. A strong argument has been made that much of the data on prion infectivity fits the template-assisted model (56). Interestingly, a prion peptide fragment PrP[109–122] was capable of converting normally  $\alpha$ -helical peptide fragments into  $\beta$ -sheet conformers (18). Similarly, proteins with extended polyglutamine regions can “recruit” proteins with normal-length polyglutamine stretches into the aggregates, even when the normal length polyglutamine proteins would not aggregate by themselves; recruitment depends on interactions between the polyglutamine domains (57). These studies further support the existence of a mechanism for induced conversion of monomer peptide to  $\beta$ -sheet aggregate.

Most likely, both spontaneous and induced conversion of monomers of A $\beta$ , PrP, and htt to  $\beta$ -sheet aggregates occur. The relative importance of the two alternative modes depends on the conformational stability of the peptide monomer, peptide concentration, the presence of pre-existing aggregated material, and the mode of presentation of aggregated material to soluble monomer (e.g., suspended or immobilized aggregates).

In one interesting model, the authors skirted the issue of kinetics of conversion and looked at the kinetics of pathogenesis, considering the kinetics of amyloid production, metabolism, and cell-to-cell transport (58). Another model postulated a mechanism by which interspecies transmission of prion disease may occur. Briefly, the formation of an intermediate conformational state from host cellular PrP ( $\text{PrP}^{\text{C}}$ ) was postulated to be catalyzed by inoculation with heterologous scrapie-form PrP ( $\text{PrP}^{\text{Sc}}$ ), with conversion of host  $\text{PrP}^{\text{C}}$  to host  $\text{PrP}^{\text{Sc}}$  catalyzed both by this intermediate and autocatalytically by  $\text{PrP}^{\text{Sc}}$  (59). Although interesting, these studies must be considered speculative rather than definitive, as many of the model parameters and even the model structure were not rigorously verified by experiment.

## ARE THE AGGREGATES TOXIC?

The conventional view has been that amyloid aggregates are pathological. Numerous studies have shown that aggregated  $A\beta$  is toxic in vitro (60, 61), and toxicity has been linked to a specific fibrillar morphology (62). More recently, however, an alternative view is emerging: that it is not the insoluble  $A\beta$  aggregates themselves, but rather an oligomeric intermediate that is the primary toxic species (49, 63–65).

In vitro toxicity of several PrP fragments has been demonstrated (66). The toxicity correlated with hydrophobicity of the core AGAAAAGA sequence (42, 67), rather than specifically  $\beta$ -sheet structure or fibrillar morphology of aggregates (67). No obligatory correlation between formation of aggregates with amyloid properties (e.g., Congo red binding, fibril morphology, protease resistance) and infectivity of scrapie prion protein fragments was observed, but the  $\beta$ -sheet content did correlate with infectivity (68). This result is consistent with the hypothesis that, for PrP also, oligomeric  $\beta$ -sheet intermediates, rather than the insoluble aggregates, are required for infectivity and/or toxicity.

There is considerable disagreement in the literature as to whether aggregates in Huntington's disease are directly toxic. Li et al. observed a strong correlation in mutant mice between production of N-terminal huntingtin fragments, aggregation, and selective neuritic degeneration (69). A different conclusion was reached in another study in which it appeared that there was no correlation between huntingtin aggregates and cell loss; in fact, it was suggested that aggregates serve a cytoprotective role (70). Inhibition of caspase reduced generation of huntingtin fragments, extent of aggregation, and toxicity (71). Intracellular deposits of aggregated htt with expanded polyglutamine domains directly inhibited normal functioning of the ubiquitin-proteasome system, an effect that could lead to cellular dysfunction and death (72). Hsp70 suppressed polyglutamine toxicity without a visible effect on aggregate formation in a fruit-fly model (73). A different conclusion came out of a study employing mammalian cells transfected with the gene encoding for the huntingtin fragment; both GroEl and Hsp104 expression reduced polyglutamine-mediated aggregation and cell toxicity (74). This remains a controversial issue [see Ref. (75) for a brief review].

## INHIBITORS OF AGGREGATION AND/OR TOXICITY

Because aggregates are associated with pathology, efforts are underway to develop compounds that interfere with aggregation of htt, PrP, and A $\beta$ , with the hope that such compounds will also prevent toxicity. Interestingly, several compounds have turned up as potentially useful against more than one of these chemically distinct peptides.

One class of promising candidates for interference of self-assembly of neuropeptides includes the sulfonated dyes Congo red and thioflavine S, both of which are used as histochemical stains for amyloid fibrils. Congo red disrupts A $\beta$  aggregation and toxicity (76, 77) and inhibits fibrillogenesis of huntingtin fragments (78). Chrysamine G, a more lipophilic variant of Congo red, was also effective against A $\beta$  (79) and huntingtin (78). Several other small molecules, typically with highly conjugated cyclic groups, have been successful to different degrees as inhibitory compounds. Daunomycin and related anthracyclines, rifampicin and related naphthahydroquinones, and benzofurans reportedly interfered with A $\beta$  aggregation and/or toxicity (80, 81). Porphyrins and phthalocyanines inhibited conversion of soluble PrP to its protease-resistant form independent of charge group (82). From a large library of imidazopyridoindoles, some compounds active against A $\beta$  were found; these compounds inhibited random coil to  $\beta$ -sheet conformational transition, inhibited aggregation, and prevented neurotoxicity (83). One interesting compound is a pyridone that enhances aggregation of both A $\beta$  and PrP fragments (84).

Another approach for inhibiting aggregate formation that has met with some success is the use of specific antibodies targeted against the peptide domain assumed to be essential for aggregation. Nuclear inclusion formation in cells was greatly reduced by coexpression of a huntingtin fragment and a single-chain Fv antibody targeted to the N-terminus of huntingtin (85). In *in vitro* studies, an antibody that recognizes only the soluble form of extended polyglutamine domains of proteins inhibited fibril formation, although significant quantities of amorphous aggregated materials were detected (78). Antibodies raised against the N-terminus of A $\beta$  prevented fibril formation *in vitro*, partially restored peptide solubility of preformed A $\beta$  fibrils, and inhibited toxicity (86).

Because the peptides under discussion are self-assembling, it may be possible to target each peptide specifically by using a short peptide fragment homologous to a segment of the full-length peptide. This idea has occurred to several groups, and implementation of the idea has met with some success. Of particular interest are those peptide-based compounds that, by binding to the self-assembling peptide, interfere with its assembly into (presumably) toxic aggregates. Furthest advanced are studies with peptide-based inhibitors of A $\beta$ . The sequence KLVFF, corresponding to residues 16–20 of A $\beta$  (the “conformationally confused” region; Figure 1B) was one of the most effective pentapeptides in binding to and inhibiting A $\beta$  aggregation (87). Several variations on this theme have been investigated with some success. Substitution of prolines for some of these residues produced “ $\beta$ -sheet breaker” peptides reportedly capable of inhibiting A $\beta$  aggregation and

toxicity (88). N-methylated A $\beta$ [25–35] peptides were able to inhibit toxicity of A $\beta$ , possibly by binding to A $\beta$  and preventing further intermolecular hydrogen bonding (89). In a slightly different approach, attachment of nonhomologous peptide sequences or other groups to the KLVFF sequence produced compounds capable of inhibiting A $\beta$  aggregation and/or toxicity (90–92). Some of the peptidyl compounds most effective at inhibiting A $\beta$  toxicity actually accelerate the A $\beta$  aggregation rate (93). This unexpected result is in line with the hypothesis that intermediates in the aggregation pathway, not the end products themselves, are the toxic moiety.

Taking a similar approach, several short peptides homologous to the central and C-terminal regions of PrP have been shown to be effective at inhibiting conversion of soluble PrP to the  $\beta$ -sheet-rich protease-resistant form (94, 95) or at inhibiting PrP toxicity in vitro (67). The mechanism of action appears to involve binding of the peptide inhibitor to the soluble form of PrP, or to cell-associated PrP. Interestingly, in one study the effective peptide inhibitors tended to form  $\beta$ -sheet-rich structures by themselves (95). A slightly different approach has been used for identifying peptidyl inhibitors for use with huntingtin. Using phage display to screen a combinatorial peptide library, Nagai and coworkers identified several tryptophan-rich 11-mers with anti-aggregation activity against poly Q-containing proteins (96).

## SUMMARY AND FUTURE DIRECTIONS

Promising advances have been made in designing compounds that specifically target self-assembling polypeptides and inhibit their adverse side effects in vitro. Bringing these compounds to the clinic requires not only development of combinatorial libraries and effective high-throughput screening methods, but also advances in our basic understanding of the conformational changes underlying conversion of monomer to aggregate, and the relationship between physicochemical properties and biological function.

**The *Annual Review of Biomedical Engineering* is online at  
<http://bioeng.annualreviews.org>**

## LITERATURE CITED

1. McGowan DP, van Roon-Mom W, Holloway H, Bates GP, Mangiarini L, et al. 2000. Amyloid-like inclusions in Huntington's disease. *Neuroscience* 100:677–80
2. Vassar R, Citron M. 2000. Abeta-generating enzymes: recent advances in beta- and gamma-secretase research. *Neuron* 27:419–22
3. Evert BO, Wullner U, Klockgether T. 2000. Cell death in polyglutamine diseases. *Cell Tissue Res*. 301:189–204
4. Mende-Mueller LM, Toneff T, Hwang SR, Chesselet MF, Hook VY. 2001. Tissue-specific proteolysis of Huntingtin (htt) in human brain: evidence of enhanced levels of N- and C-terminal htt



- fragments in Huntington's disease striatum. *J. Neurosci.* 21:1830–37
5. Caughey B. 2000. Transmissible spongiform encephalopathies, amyloidoses and yeast prions: common threads? *Nat. Med.* 6:751–54
  6. Kallberg Y, Gustafsson M, Persson B, Thyberg J, Johansson J. 2001. Prediction of amyloid fibril-forming proteins. *J. Biol. Chem.* 276:12945–50
  7. Chiti F, Taddei N, Bucciantini M, White P, Ramponi G, Dobson CM. 2000. Mutational analysis of the propensity for amyloid formation by a globular protein. *EMBO J.* 19:1441–49
  8. West MW, Wang W, Patterson J, Mancias JD, Beasley JR, Hecht MH. 1999. De novo amyloid proteins from designed combinatorial libraries. *Proc. Natl. Acad. Sci. USA* 96:11211–16
  9. Barrow CJ, Yasuda A, Kenny PT, Zagorski MG. 1992. Solution conformations and aggregational properties of synthetic amyloid beta-peptides of Alzheimer's disease. Analysis of circular dichroism spectra. *J. Mol. Biol.* 225:1075–93
  10. Talafoos J, Marcinowski KJ, Klopman G, Zagorski MG. 1994. Solution structure of residues 1–28 of the amyloid beta-peptide. *Biochemistry* 33:7788–96
  11. Kohno T, Kobayashi K, Maeda T, Sato K, Takashima A. 1996. Three-dimensional structures of the amyloid beta peptide (25–35) in membrane-mimicking environment. *Biochemistry* 35:16094–104
  12. Fraser PE, Nguyen JT, Surewicz WK, Kirschner DA. 1991. pH-dependent structural transitions of Alzheimer amyloid peptides. *Biophys. J.* 60:1190–201
  13. Fraser PE, McLachlan DR, Surewicz WK, Mizzen CA, Snow AD, et al. 1994. Conformation and fibrillogenesis of Alzheimer A beta peptides with selected substitution of charged residues. *J. Mol. Biol.* 244:64–73
  14. Zhang Y, Swietnicki W, Zagorski MG, Surewicz WK, Sonnichsen FD. 2000. Solution structure of the E200K variant of human prion protein. Implications for the mechanism of pathogenesis in familial prion diseases. *J. Biol. Chem.* 275:33650–54
  15. Massi F, Peng JW, Lee JP, Straub JE. 2001. Simulation study of the structure and dynamics of the Alzheimer's amyloid peptide congener in solution. *Biophys. J.* 80:31–44
  16. Ragg E, Tagliavini F, Malesani P, Monticelli L, Bugiani O, et al. 1999. Determination of solution conformations of PrP106–126, a neurotoxic fragment of prion protein, by <sup>1</sup>H NMR and restrained molecular dynamics. *Eur. J. Biochem.* 266:1192–200
  17. De Gioia L, Selvaggini C, Ghibaudi E, Diomede L, Bugiani O, et al. 1994. Conformational polymorphism of the amyloidogenic and neurotoxic peptide homologous to residues 106–126 of the prion protein. *J. Biol. Chem.* 269:7859–62
  18. Nguyen J, Baldwin MA, Cohen FE, Prusiner SB. 1995. Prion protein peptides induce  $\alpha$ -helix to  $\beta$ -sheet conformational transition. *Biochemistry* 34:4186–92
  19. Zahn R, Liu A, Luhrs T, Riek R, von Schroetter C, et al. 2000. NMR solution structure of the human prion protein. *Proc. Natl. Acad. Sci. USA* 97:145–50
  20. Thompson A, White AR, McLean C, Masters CL, Cappai R, Barrow CJ. 2000. Amyloidogenicity and neurotoxicity of peptides corresponding to the helical regions of PrP(C). *J. Neurosci. Res.* 62:293–301
  21. Swietnicki W, Morillas M, Chen SG, Gambetti P, Surewicz WK. 2000. Aggregation and fibrillization of the recombinant human prion protein huPrP90–231. *Biochemistry* 39:424–31
  22. Salmona M, Malesani P, De Gioia L, Gorla S, Bruschi M, et al. 1999. Molecular determinants of the physicochemical properties of a critical prion protein region comprising residues 106–126. *Biochem. J.* 342:207–14
  23. Hosszu LL, Baxter NJ, Jackson GS,

- Power A, Clarke AR, et al. 1999. Structural mobility of the human prion protein probed by backbone hydrogen exchange. *Nat. Struct. Biol.* 6:740–43
24. Maiti NR, Surewicz WK. 2001. The role of disulfide bridge in the folding and stability of the recombinant human prion protein. *J. Biol. Chem.* 276:2427–31
25. Jackson GS, Hosszu LL, Power A, Hill AF, Kenney J, et al. 1999. Reversible conversion of monomeric human prion protein between native and fibrillogenic conformations. *Science* 283:1935–37
26. Guilbert C, Ricard F, Smith JC. 2000. Dynamic simulation of the mouse prion protein. *Biopolymers* 54:406–15
27. Inouye H, Bond J, Baldwin MA, Ball HL, Prusiner SB, Kirschner DA. 2000. Structural changes in a hydrophobic domain of the prion protein induced by hydration and by Ala → Val and Pro → Leu substitutions. *J. Mol. Biol.* 300:1283–96
28. Perutz MF, Johnson T, Suzuki M, Finch JT. 1994. Glutamine repeats as polar zippers: their possible role in inherited neurodegenerative diseases. *Proc. Natl. Acad. Sci. USA* 91:5355–58
29. Monoi H, Futaki S, Kugimiya S, Minakata H, Yoshihara K. 2000. Poly-L-glutamine forms cation channels: relevance to the pathogenesis of the polyglutamine diseases. *Biophys. J.* 78:2892–99
30. Fraser PE, Duffy LK, O'Malley MB, Nguyen J, Inouye H, Kirschner DA. 1991. Morphology and antibody recognition of synthetic beta-amyloid peptides. *J. Neurosci. Res.* 28:474–85
31. Stine WB Jr, Snyder SW, Lador US, Wade WS, Miller MF, et al. 1996. The nanometer-scale structure of amyloid-beta visualized by atomic force microscopy. *J. Protein Chem.* 15:193–203
32. Harper JD, Wong SS, Lieber CM, Lansbury PT Jr. 1999. Assembly of A beta amyloid protofibrils: an in vitro model for a possible early event in Alzheimer's disease. *Biochemistry* 38:8972–80
33. Blackley HK, Sanders GH, Davies MC, Roberts CJ, Tendler SJ, Wilkinson MJ. 2000. In-situ atomic force microscopy study of beta-amyloid fibrillization. *J. Mol. Biol.* 298:833–40
34. Malinchik SB, Inouye H, Szumowski KE, Kirschner DA. 1998. Structural analysis of Alzheimer's beta(1-40) amyloid: protofilament assembly of tubular fibrils. *Biophys. J.* 74:537–45A
35. Kheterpal I, Zhou S, Cook KD, Wetzel R. 2000. Abeta amyloid fibrils possess a core structure highly resistant to hydrogen exchange. *Proc. Natl. Acad. Sci. USA* 97:13597–601
36. Tjernberg LO, Callaway DJ, Tjernberg A, Hahne S, Lilliehook C, et al. 1999. A molecular model of Alzheimer amyloid beta-peptide fibril formation. *J. Biol. Chem.* 274:12619–25
37. Serpell LC, Blake CC, Fraser PE. 2000. Molecular structure of a fibrillar Alzheimer's A beta fragment. *Biochemistry* 39:13269–75
38. Benzinger TL, Gregory DM, Burkoth TS, Miller-Auer H, Lynn DG, et al. 2000. Two-dimensional structure of beta-amyloid(10-35) fibrils. *Biochemistry* 39:3491–99
39. Antzutkin ON, Balbach JJ, Leapman RD, Rizzo NW, Reed J, Tycko R. 2000. Multiple quantum solid-state NMR indicates a parallel, not antiparallel, organization of beta-sheets in Alzheimer's beta-amyloid fibrils. *Proc. Natl. Acad. Sci. USA* 97:13045–50
40. Forloni G, Angeretti N, Chiesa R, Monzani E, Salmona M, et al. 1993. Neurotoxicity of a prion protein fragment. *Nature* 362:543–46
41. Baskakov IV, Legname G, Prusiner SB, Cohen FE. 2001. Folding of prion protein to its native alpha-helical conformation is under kinetic control. *J. Biol. Chem.* 276:19687–90
42. Jobling MF, Stewart LR, White AR, McLean C, Friedhuber A, et al. 1999. The hydrophobic core sequence modulates the

- neurotoxic and secondary structure properties of the prion peptide 106–126. *J. Neurochem.* 73:1557–65
43. Scherzinger E, Sittler A, Schweiger K, Heiser V, Lurz R, et al. 1999. Self-assembly of polyglutamine-containing huntingtin fragments into amyloid-like fibrils: implications for Huntington's disease pathology. *Proc. Natl. Acad. Sci. USA* 96:4604–9
44. Jarrett JT, Berger EP, Lansbury PT Jr. 1993. The C-terminus of the beta protein is critical in amyloidogenesis. *Ann. NY Acad. Sci.* 695:144–48
45. Tanski SJ, Murphy RM. 1992. Kinetics of aggregation of synthetic beta-amyloid peptide. *Arch. Biochem. Biophys.* 294:630–38
46. Snyder SW, Lador US, Wade WS, Wang GT, Barrett LW, et al. 1994. Amyloid-beta aggregation: selective inhibition of aggregation in mixtures of amyloid with different chain lengths. *Biophys. J.* 67:1216–28
47. Lomakin A, Teplow DB, Kirschner DA, Benedek GB. 1997. Kinetic theory of fibrillogenesis of amyloid beta-protein. *Proc. Natl. Acad. Sci. USA* 94:7942–47
48. Inouye H, Kirschner DA. 2000. A beta fibrillogenesis: kinetic parameters for fibril formation from congo red binding. *J. Struct. Biol.* 130:123–29
49. Pallitto MM, Murphy RM. 2001. A mathematical model of the kinetics of beta-amyloid fibril growth from the denatured state. *Biophys. J.* 81:1805–22
50. Post K, Pitschke M, Schafer O, Wille H, Appel TR, et al. 1998. Rapid acquisition of beta-sheet structure in the prion protein prior to multimer formation. *Biol. Chem.* 379:1307–17
51. Wildegger G, Liemann S, Glockshuber R. 1999. Extremely rapid folding of the C-terminal domain of the prion protein without kinetic intermediates. *Nat. Struct. Biol.* 6:550–53
52. Harrison PM, Chan HS, Prusiner SB, Cohen FE. 2001. Conformational propagation with prion-like characteristics in a simple model of protein folding. *Protein Sci.* 10:819–35
53. Tseng BP, Esler WP, Clish CB, Stimson ER, Ghilardi JR, et al. 1999. Deposition of monomeric, not oligomeric, Abeta mediates growth of Alzheimer's disease amyloid plaques in human brain preparations. *Biochemistry* 38:10424–31
54. Esler WP, Stimson ER, Jennings JM, Vinters HV, Ghilardi JR, et al. 2000. Alzheimer's disease amyloid propagation by a template-dependent dock-lock mechanism. *Biochemistry* 39:6288–95
55. Esler WP, Felix AM, Stimson ER, Lachenmann MJ, Ghilardi JR, et al. 2000. Activation barriers to structural transition determine deposition rates of Alzheimer's disease a beta amyloid. *J. Struct. Biol.* 130:174–83
56. Cohen FE, Prusiner SB. 1998. Pathologic conformations of prion proteins. *Annu. Rev. Biochem.* 67:793–819
57. Kazantsev A, Preisinger E, Dranovsky A, Goldgaber D, Housman D. 1999. Insoluble detergent-resistant aggregates form between pathological and nonpathological lengths of polyglutamine in mammalian cells. *Proc. Natl. Acad. Sci. USA* 96:11404–9
58. Stumpf MP, Krakauer DC. 2000. Mapping the parameters of prion-induced neuropathology. *Proc. Natl. Acad. Sci. USA* 97:10573–77
59. Kellershohn N, Laurent M. 1998. Species barrier in prion diseases: a kinetic interpretation based on the conformational adaptation of the prion protein. *Biochem. J.* 334:539–45
60. Pike CJ, Burdick D, Walencewicz AJ, Glabe CG, Cotman CW. 1993. Neurodegeneration induced by beta-amyloid peptides in vitro: the role of peptide assembly state. *J. Neurosci.* 13:1676–87
61. Shearman MS, Ragan CI, Iversen LL. 1994. Inhibition of PC12 cell redox activity is a specific, early indicator of the mechanism of beta-amyloid-mediated

- cell death. *Proc. Natl. Acad. Sci. USA* 91: 1470–74
62. Seilheimer B, Bohrmann B, Bondolfi L, Muller F, Stuber D, Dobeli H. 1997. The toxicity of the Alzheimer's beta-amyloid peptide correlates with a distinct fiber morphology. *J. Struct. Biol.* 119:59–71
63. Roher AE, Chaney MO, Kuo YM, Webster SD, Stine WB, et al. 1996. Morphology and toxicity of Abeta-(1-42) dimer derived from neuritic and vascular amyloid deposits of Alzheimer's disease. *J. Biol. Chem.* 271:20631–35
64. Hartley DM, Walsh DM, Ye CP, Diehl T, Vasquez S, et al. 1999. Protofibrillar intermediates of amyloid beta-protein induce acute electrophysiological changes and progressive neurotoxicity in cortical neurons. *J. Neurosci.* 19:8876–84
65. Ward RV, Jennings KH, Jepras R, Neville W, Owen DE, et al. 2000. Fractionation and characterization of oligomeric, protofibrillar and fibrillar forms of beta-amyloid peptide. *Biochem. J.* 348(Pt 1): 137–44
66. Ettaiche M, Pichot R, Vincent JP, Chabry J. 2000. In vivo cytotoxicity of the prion protein fragment 106-126. *J. Biol. Chem.* 275:36487–90
67. Brown DR. 2000. Prion protein peptides: optimal toxicity and peptide blockade of toxicity. *Mol. Cell Neurosci.* 15:66–78
68. Wille H, Prusiner SB, Cohen FE. 2000. Scrapie infectivity is independent of amyloid staining properties of the N-terminally truncated prion protein. *J. Struct. Biol.* 130:323–38
69. Li H, Li SH, Johnston H, Shelbourne PF, Li XJ. 2000. Amino-terminal fragments of mutant huntingtin show selective accumulation in striatal neurons and synaptic toxicity. *Nat. Genet.* 25:385–89
70. Kuemmerle S, Gutekunst CA, Klein AM, Li XJ, Li SH, et al. 1999. Huntingtin aggregates may not predict neuronal death in Huntington's disease. *Ann. Neurol.* 46: 842–49
71. Wellington CL, Singaraja R, Ellerby L, Savill J, Roy S, et al. 2000. Inhibiting caspase cleavage of huntingtin reduces toxicity and aggregate formation in neuronal and nonneuronal cells. *J. Biol. Chem.* 275:19831–38
72. Bence NF, Sampat RM, Kopito RR. 2001. Impairment of the ubiquitin-proteasome system by protein aggregation. *Science* 292:1552–55
73. Warrick JM, Chan HY, Gray-Board GL, Chai Y, Paulson HL, Bonini NM. 1999. Suppression of polyglutamine-mediated neurodegeneration in *Drosophila* by the molecular chaperone HSP70. *Nat. Genet.* 23:425–28
74. Carmichael J, Chatellier J, Woolfson A, Milstein C, Fersht AR, Rubinsztein DC. 2000. Bacterial and yeast chaperones reduce both aggregate formation and cell death in mammalian cell models of Huntington's disease. *Proc. Natl. Acad. Sci. USA* 97:9701–5
75. Ferrigno P, Silver PA. 2000. Polyglutamine expansions: proteolysis, chaperones, and the dangers of promiscuity. *Neuron* 26:9–12
76. Kisilevsky R, Lemieux LJ, Fraser PE, Kong X, Hultin PG, Szarek WA. 1995. Arresting amyloidosis in vivo using small-molecule anionic sulphonates or sulphates: implications for Alzheimer's disease. *Nat. Med.* 1:143–48
77. Lorenzo A, Yankner BA. 1994. Beta-amyloid neurotoxicity requires fibril formation and is inhibited by congo red. *Proc. Natl. Acad. Sci. USA* 91:12243–47
78. Heiser V, Scherzinger E, Boeddrich A, Nordhoff E, Lurz R, et al. 2000. Inhibition of huntingtin fibrillogenesis by specific antibodies and small molecules: implications for Huntington's disease therapy. *Proc. Natl. Acad. Sci. USA* 97:6739–44
79. Klunk WE, Debnath ML, Koros AM, Pettegrew JW. 1998. Chrysamine-G, a lipophilic analogue of Congo red, inhibits A beta-induced toxicity in PC12 cells. *Life Sci.* 63:1807–14

80. Howlett DR, Perry AE, Godfrey F, Swatton JE, Jennings KH, et al. 1999. Inhibition of fibril formation in beta-amyloid peptide by a novel series of benzofurans. *Biochem. J.* 340:283–89
81. Tomiyama T, Shoji A, Kataoka K, Suwa Y, Asano S, et al. 1996. Inhibition of amyloid beta protein aggregation and neurotoxicity by rifampicin. Its possible function as a hydroxyl radical scavenger. *J. Biol. Chem.* 271:6839–44
82. Caughey WS, Raymond LD, Horiuchi M, Caughey B. 1998. Inhibition of protease-resistant prion protein formation by porphyrins and phthalocyanines. *Proc. Natl. Acad. Sci. USA* 95:12117–22
83. Reixach N, Crooks E, Ostresh JM, Houghten RA, Blondelle SE. 2000. Inhibition of beta-amyloid-induced neurotoxicity by imidazopyridindoles derived from a synthetic combinatorial library. *J. Struct. Biol.* 130:247–58
84. Kuner P, Bohrmann B, Tjernberg LO, Naslund J, Huber G, et al. 2000. Controlling polymerization of beta-amyloid and prion-derived peptides with synthetic small molecule ligands. *J. Biol. Chem.* 275:1673–78
85. Lecerf JM, Shirley TL, Zhu Q, Kazantsev A, Amersdorfer P, et al. 2001. Human single-chain Fv intrabodies counteract in situ huntingtin aggregation in cellular models of Huntington's disease. *Proc. Natl. Acad. Sci. USA* 98:4764–69
86. Solomon B, Koppel R, Frankel D, Hanan-Aharon E. 1997. Disaggregation of Alzheimer beta-amyloid by site-directed mAb. *Proc. Natl. Acad. Sci. USA* 94:4109–12
87. Tjernberg LO, Naslund J, Lindqvist F, Johansson J, Karlstrom AR, et al. 1996. Arrest of beta-amyloid fibril formation by a pentapeptide ligand. *J. Biol. Chem.* 271:8545–48
88. Soto C, Sigurdsson EM, Morelli L, Kumar RA, Castano EM, Frangione B. 1998. Beta-sheet breaker peptides inhibit fibrillogenesis in a rat brain model of amyloidosis: implications for Alzheimer's therapy. *Nat. Med.* 4:822–26
89. Hughes E, Burke RM, Doig AJ. 2000. Inhibition of toxicity in the beta-amyloid peptide fragment beta-(25–35) using N-methylated derivatives: a general strategy to prevent amyloid formation. *J. Biol. Chem.* 275:25109–15
90. Ghanta J, Shen CL, Kiessling LL, Murphy RM. 1996. A strategy for designing inhibitors of beta-amyloid toxicity. *J. Biol. Chem.* 271:29525–28
91. Findeis MA, Musso GM, Arico-Muendel CC, Benjamin HW, Hundal AM, et al. 1999. Modified-peptide inhibitors of amyloid beta-peptide polymerization. *Biochemistry* 38:6791–800
92. Pallitto MM, Ghanta J, Heinzelman P, Kiessling LL, Murphy RM. 1999. Recognition sequence design for peptidyl modulators of beta-amyloid aggregation and toxicity. *Biochemistry* 38:3570–78
93. Lowe TL, Strzelec A, Kiessling LL, Murphy RM. 2001. Structure-function relationships for inhibitors of beta-amyloid toxicity containing the recognition sequence KLVFF. *Biochemistry* 40:7882–89
94. Chabry J, Priola SA, Wehrly K, Nishio J, Hope J, Chesebro B. 1999. Species-independent inhibition of abnormal prion protein (PrP) formation by a peptide containing a conserved PrP sequence. *J. Virol.* 73:6245–50
95. Horiuchi M, Baron GS, Xiong LW, Caughey B. 2001. Inhibition of interactions and interconversions of prion protein isoforms by peptide fragments from the C-terminal folded domain. *J. Biol. Chem.* 276:15489–97
96. Nagai Y, Tucker T, Ren H, Kenan DJ, Henderson BS, et al. 2000. Inhibition of polyglutamine protein aggregation and cell death by novel peptides identified by phage display screening. *J. Biol. Chem.* 275:10437–42